Magnetic Reconnection in Realistically Turbulent Astrophysical Media

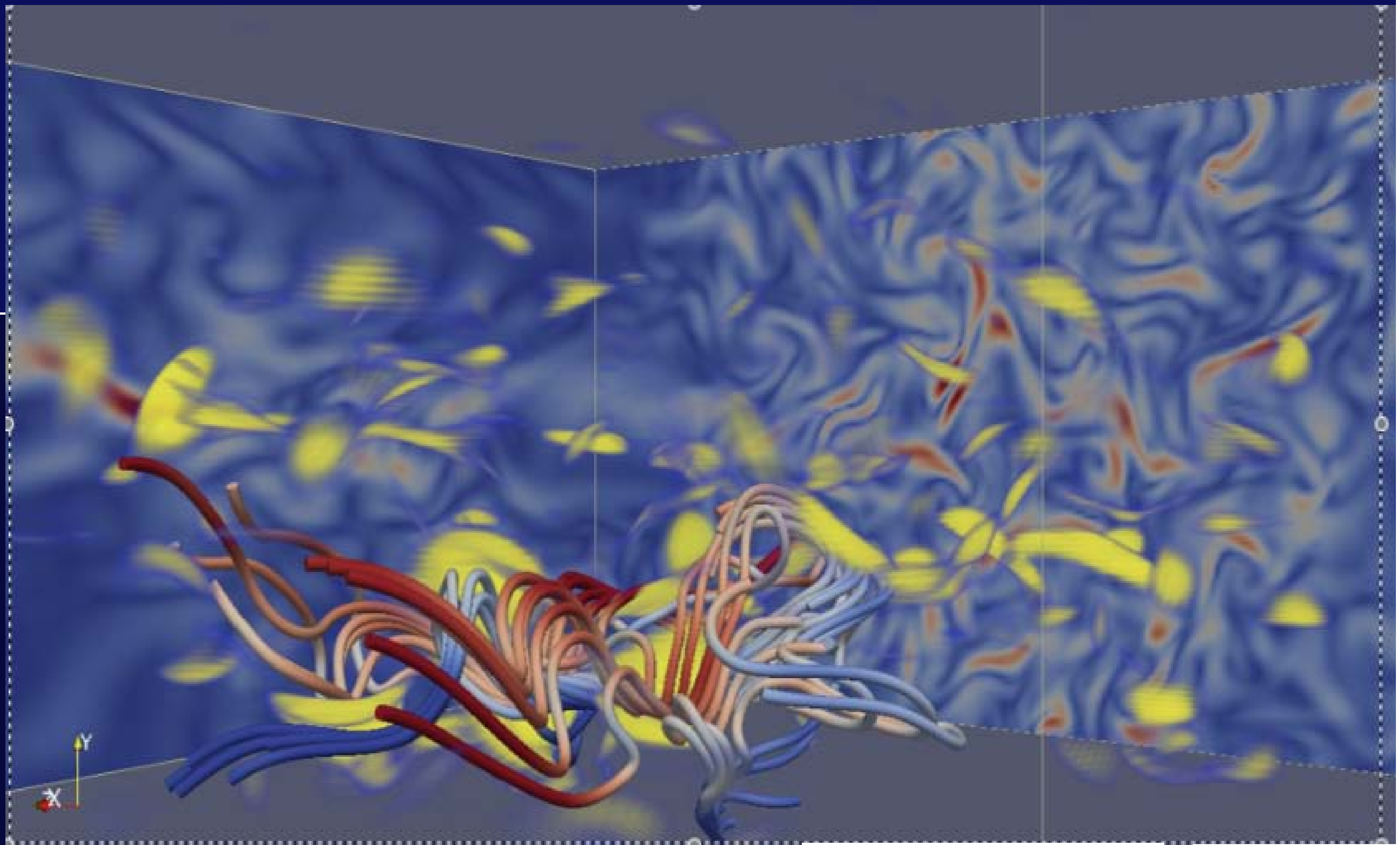

Alex Lazarian

Collaboration: G. Kowal, E. Vishniac,
E. Gouveia dal Pino, K. Otminowska-Mazur

Alexander von Humboldt Stiftung/Foundation

THE UNIVERSITY of WISCONSIN MADISON

Astrophysical reconnection was always associated with a particular kind of waves

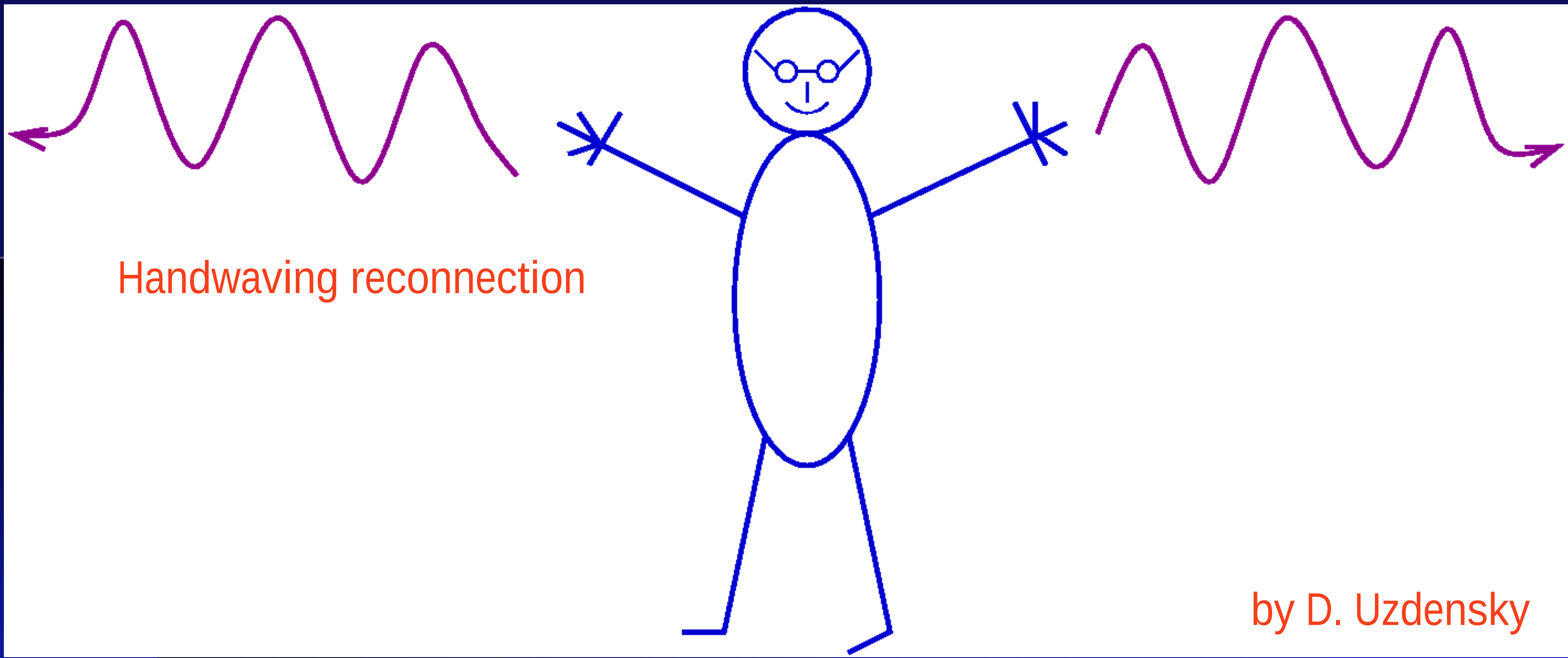

It is good to see whether other types of waves or non-linear interactions can do the job

Part I. Is turbulence ubiquitous in Astrophysics?

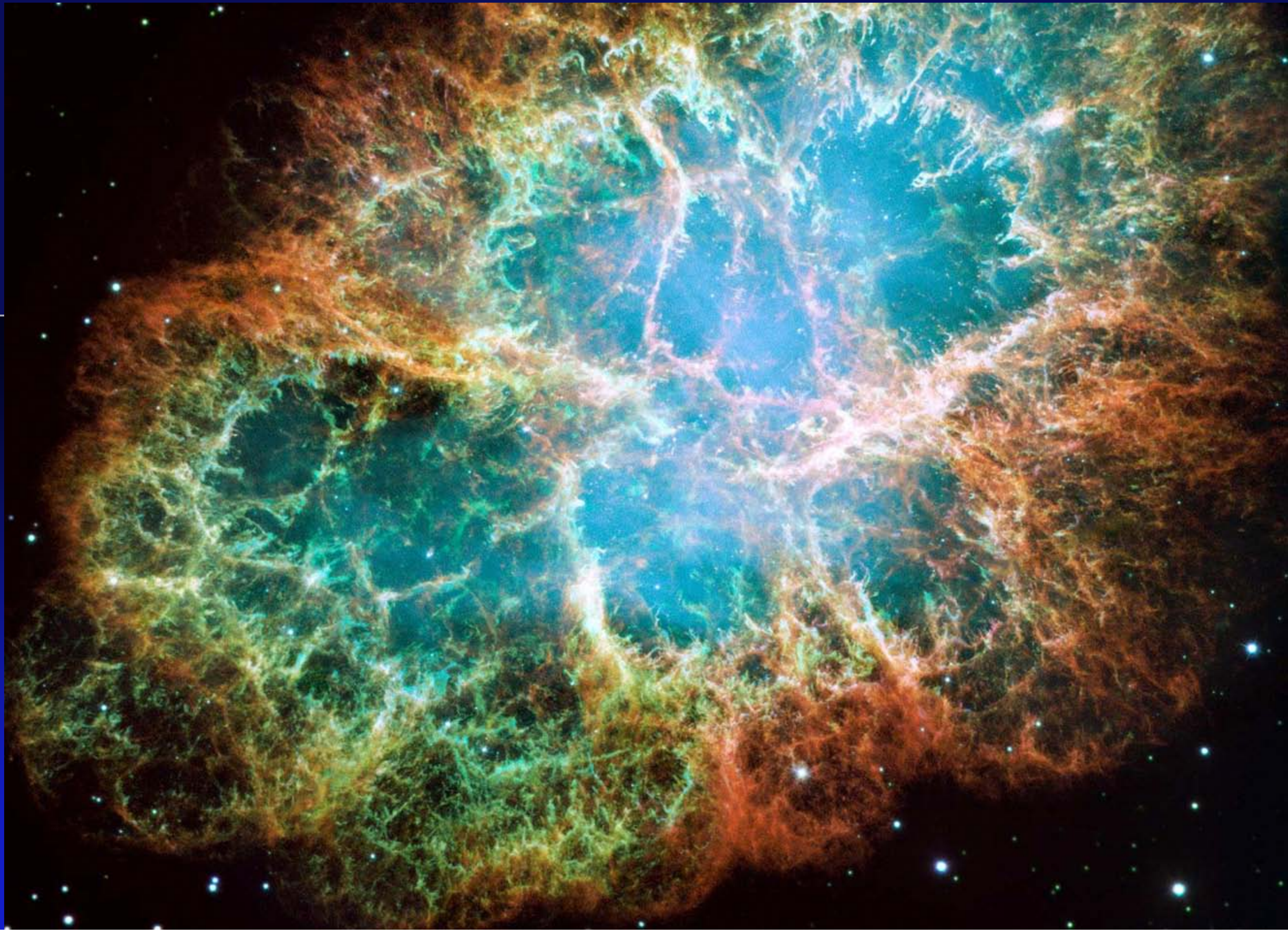

Kolmogorov theory reveals order in chaos for incompressible hydro turbulence

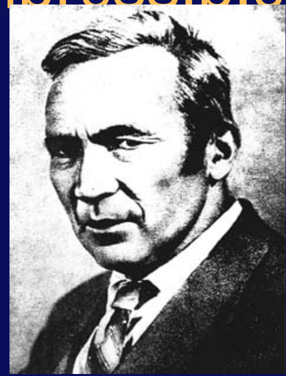

$$\left.\begin{aligned} \frac{V_l^{\,2}}{t_{cas,l}} &= \text{const} \\ t_{cas,l} &= l/V_l \end{aligned}\right\} \quad \frac{V_l^{\,3}}{l} = \text{const},\ V_l \sim l^{1/3}$$

Or, $E(k) \sim k^{-5/3}$

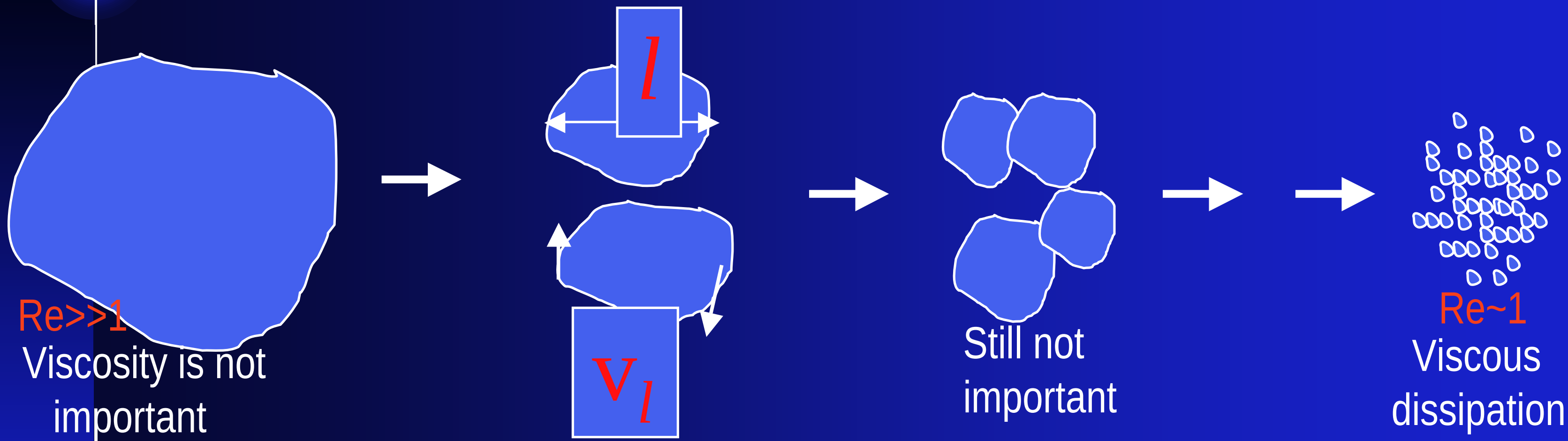

Spacecraft measurements reveal power-law spectra of fluctuations

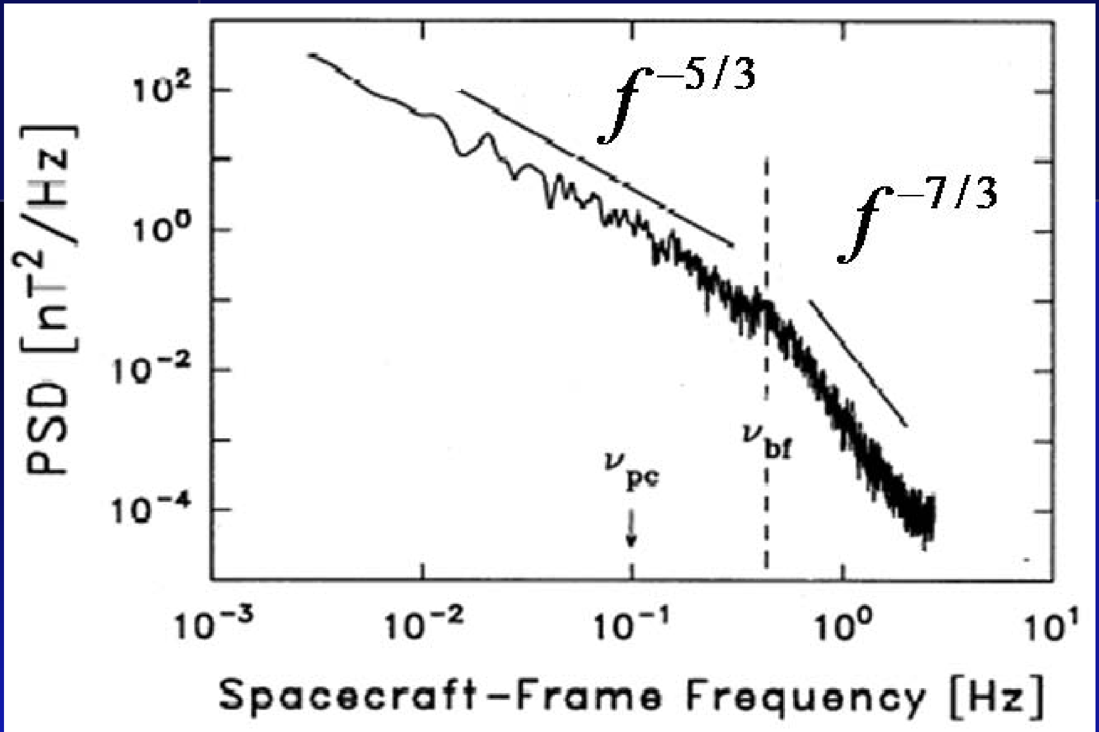

R.J. Leamon et al., JGR (1998)

- two power laws: attributed to "Inertial range" & "Dispersive range"
- break in the vicinity of the proton cyclotron frequency

Spectra of EMHD Turbulence corresponds to the expected $E_b \sim k^{-7/3}$

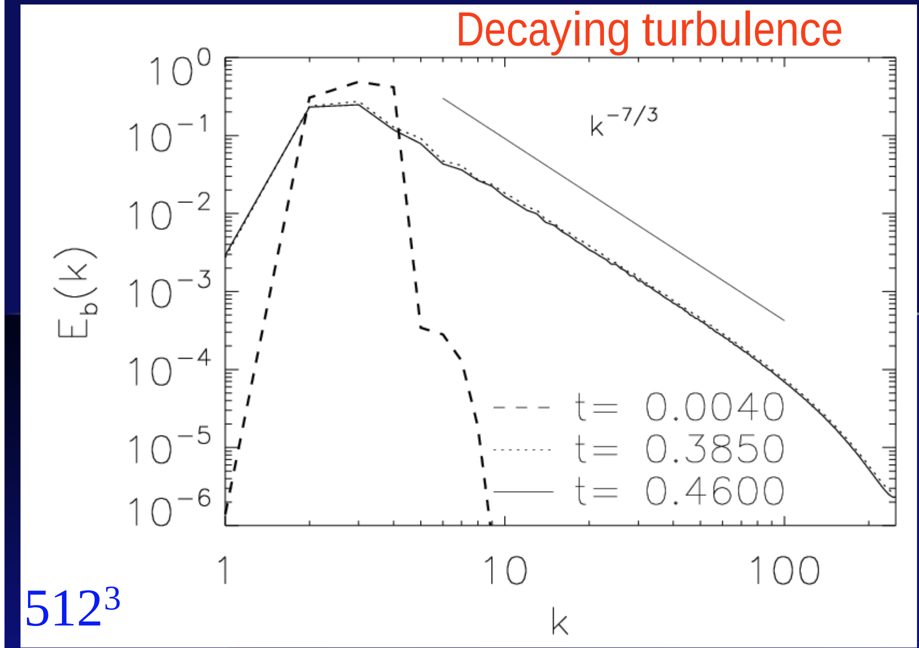

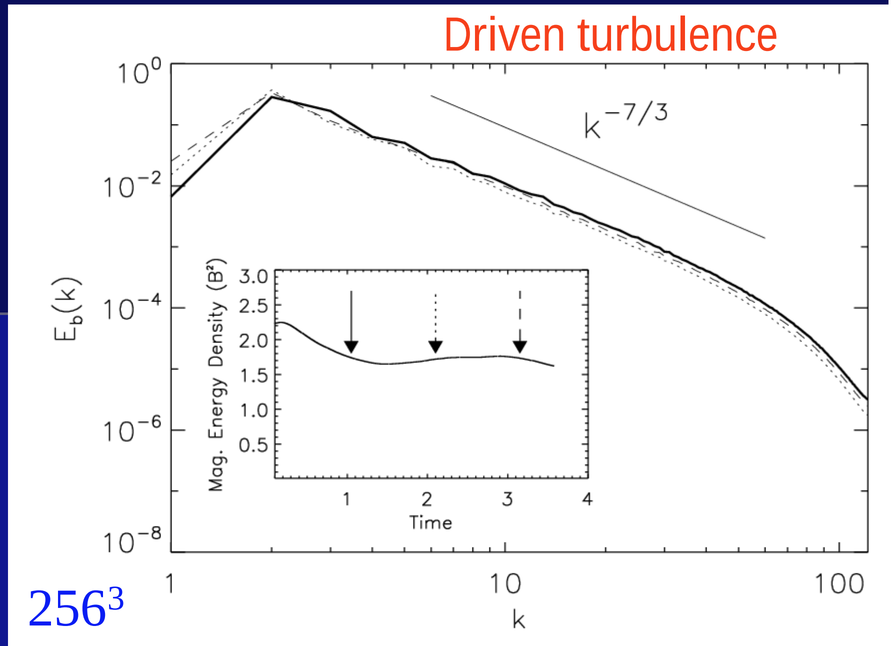

Cho & Lazarian 09

Correspond to results of Biskamp & Drake in late 90s and also to more recent calculations in Cho & Lazarian 04, Howes et al. 08

ISM reveals Kolmogorov spectrum of density fluctuations.

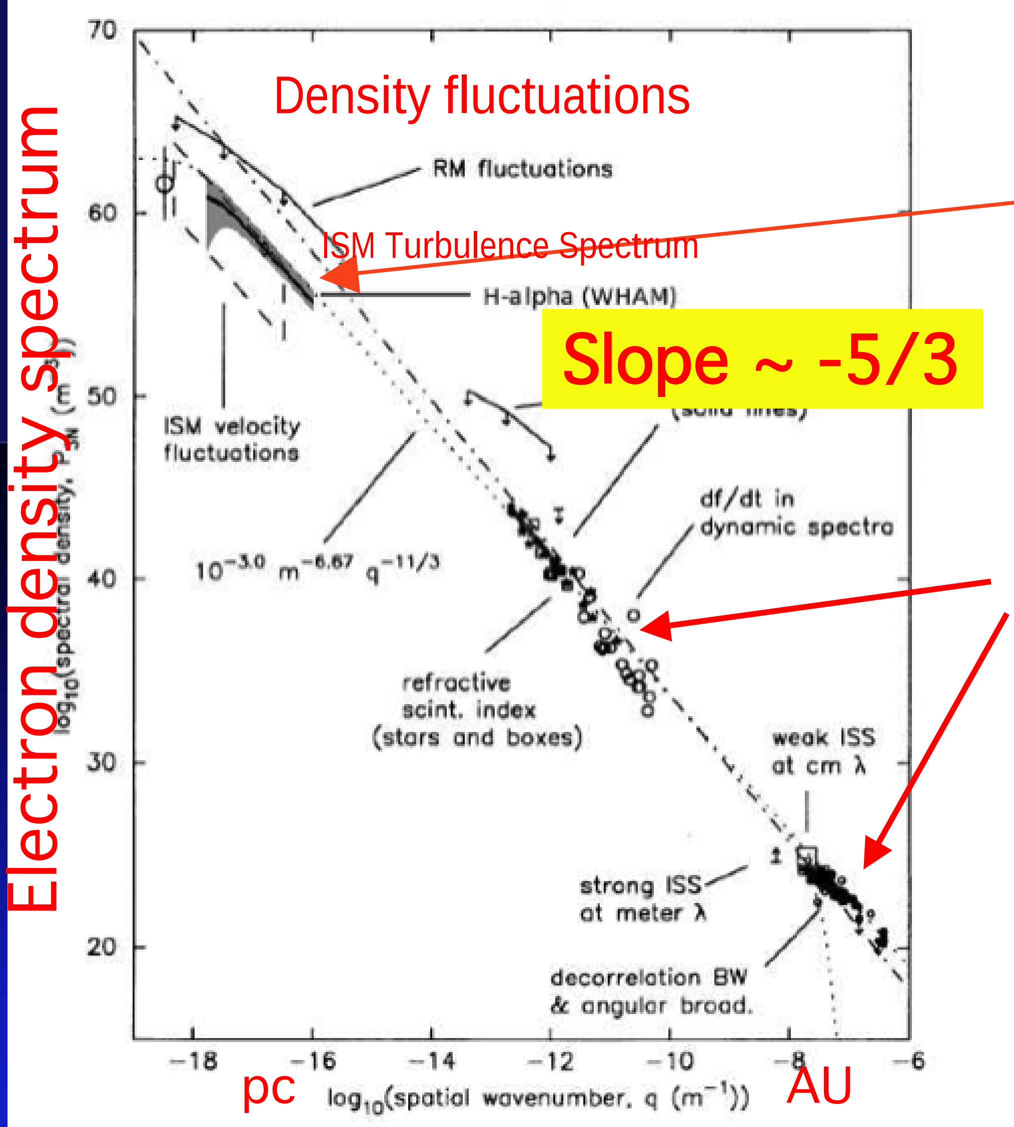

Fig. 5.— WHAM estimation for electron density overplotted on the figure of the Big Power Law in the sky figure from Armstrong et al. (1995). The range of statistical errors is marked with the gray color.

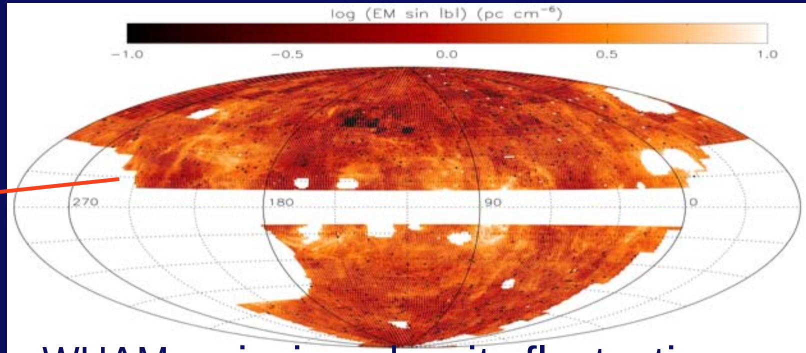

WHAM emission: density fluctuations

Chepurnov & Lazarian 2010

Scincillations and scattering

Turbulence broadens emission and absorption lines and this can be used to study turbulence with VCA techniques

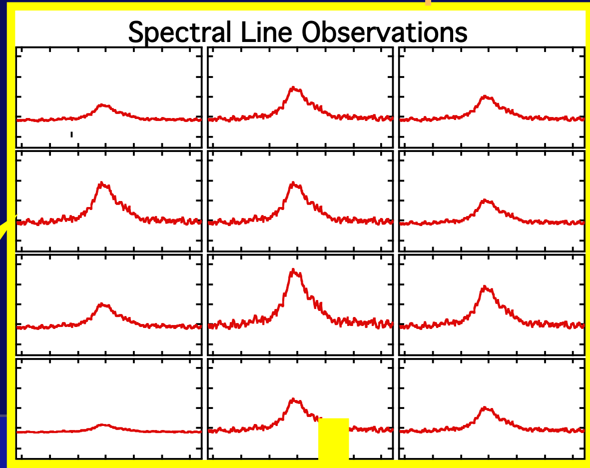

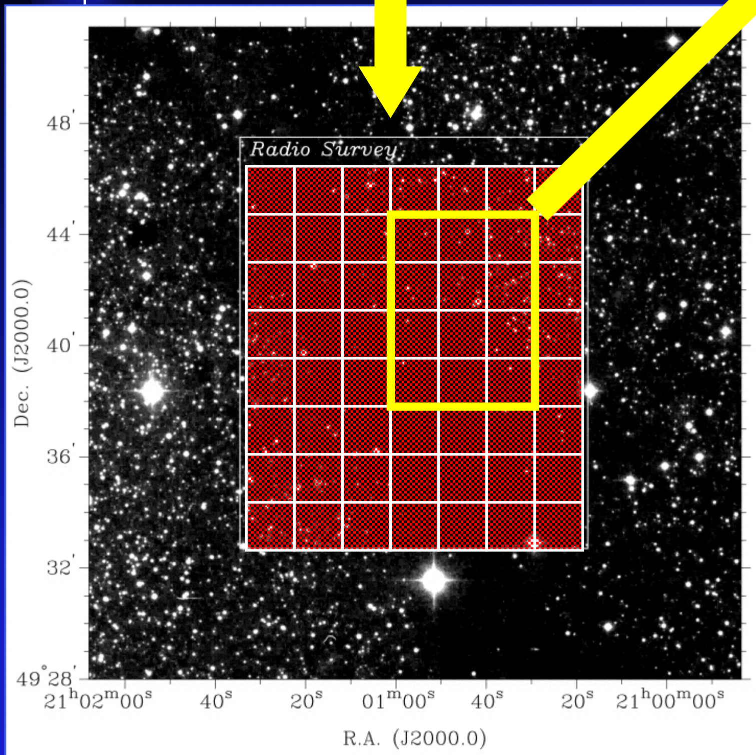

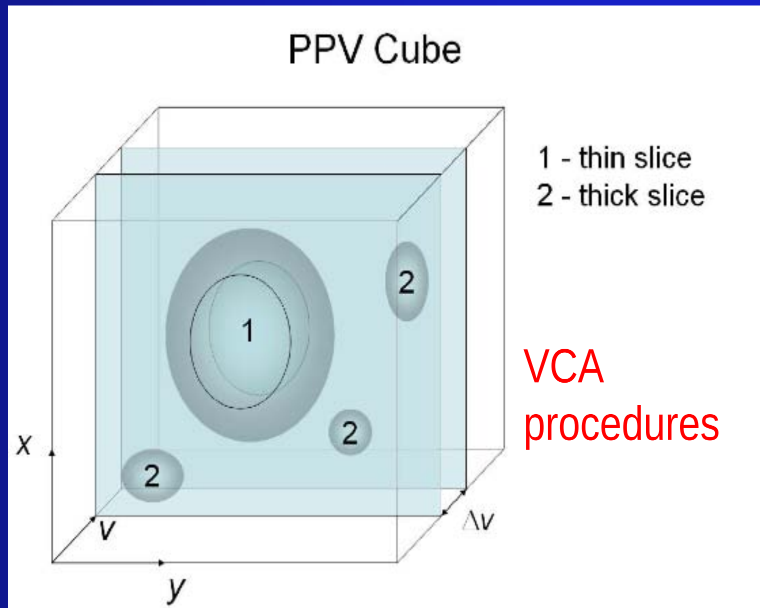

Developed in Lazarian & Pogosyan 00, 04

Mathematical Setting

Brace yourself, marshal all your strength

Nahum 2:1

$$\rho_s(\mathbf{X},v)\mathrm{d}\mathbf{X}dv = \left[\int_0^S \mathrm{d}z\; \rho(\mathbf{x})\phi_v(\mathbf{x})\right]\mathrm{d}\mathbf{X}dv$$

Density in PPV

$$\phi_v(\mathbf{x})\mathrm{d}v = \frac{1}{(2\pi\beta)^{1/2}}\exp\left[-\frac{(v-v_{gal}(\mathbf{x})-u(\mathbf{x}))^2}{2\beta}\right]\mathrm{d}v$$

Velocity distribution

$$\xi_s(R,v_1,v_2)\equiv\langle\rho_s(\mathbf{X}_1,v_1)\rho_s(\mathbf{X}_2,v_2)\rangle$$

Correlation function in PPV

$$\xi_s(\mathbf{R},v)\sim\int dz\,\frac{\xi(\mathbf{r})}{(D_z(\mathbf{r})+2\beta)^{1/2}}\exp\left[\frac{v^2}{2(D_z(\mathbf{r})+2\beta)}\right]$$

where

$$\xi(\mathbf{r}) = \langle\rho(\mathbf{x})\rho(\mathbf{x}+\mathbf{r})\rangle\propto 1+(r/r_0)^\gamma$$

Real (xyz) density correlation

$$D_z(\mathbf{r})\propto r^m$$

Velocity correlation, m=2/3 for Kolmogorov

Lazarian & Pogosyan 00

Example of the procedure application to ^{18}CO in L1551

$$-3-\gamma+m/2 \approx -2.44 \Longrightarrow m \approx 0.72$$

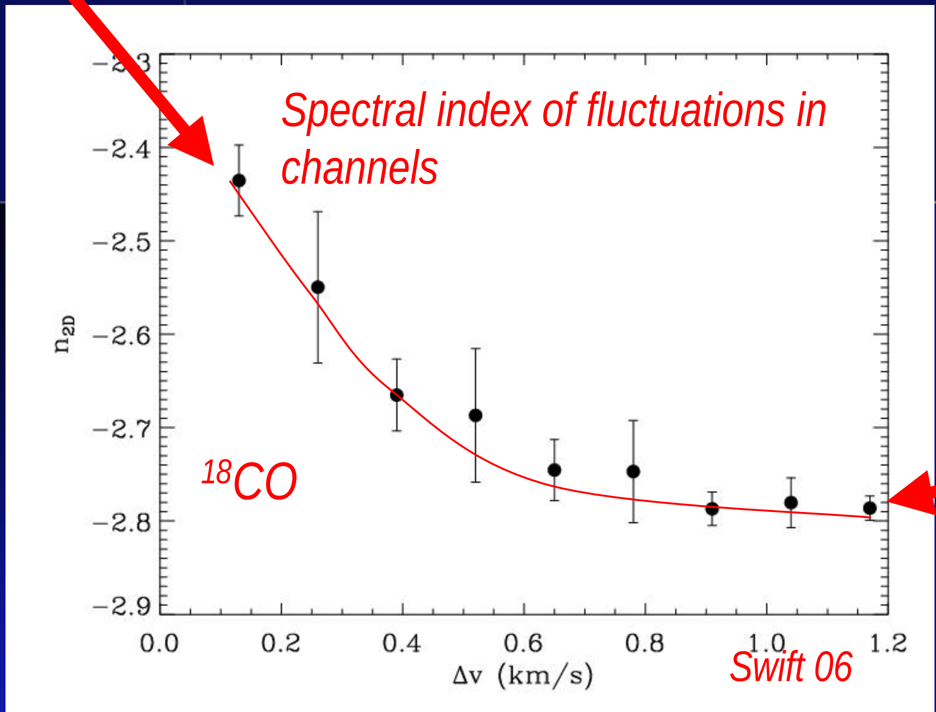

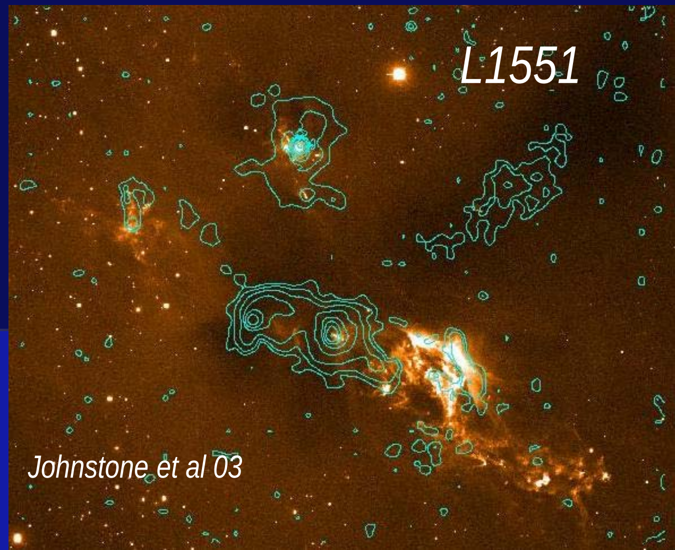

$$-3-\gamma \approx -2.8 \Longrightarrow \gamma \approx -0.2$$

Swift 06 applied VCA to ^{18}CO and obtained density spectrum $E_n(k) \sim k^{-0.8}$ and velocity spectrum $E_v \sim k^{-1.7}$.

Sparsely sampled data can be studied with our VCS techniques

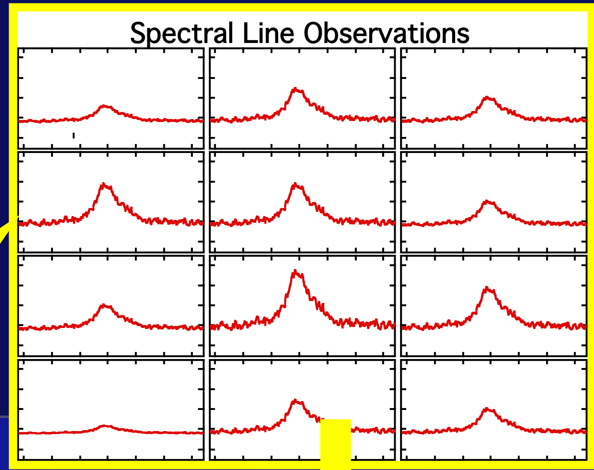

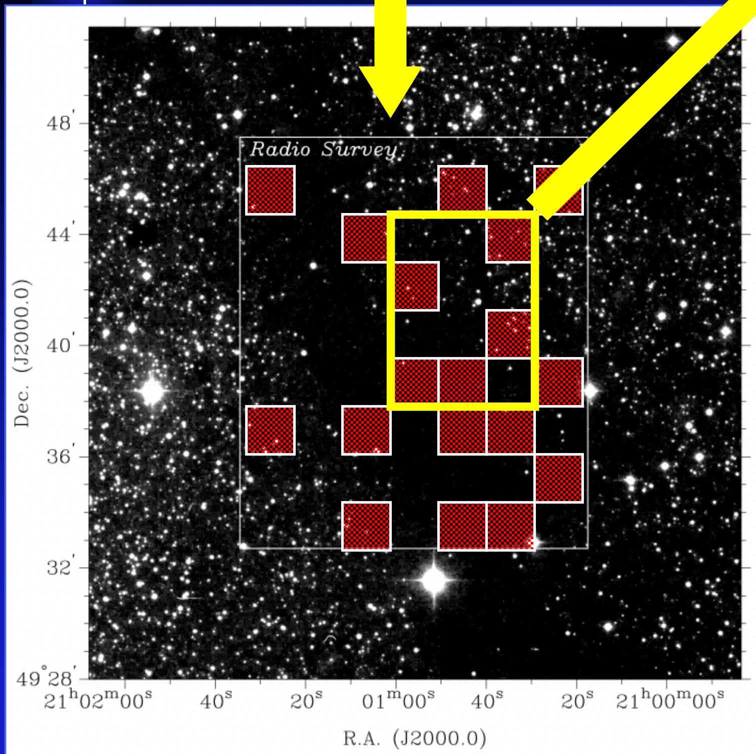

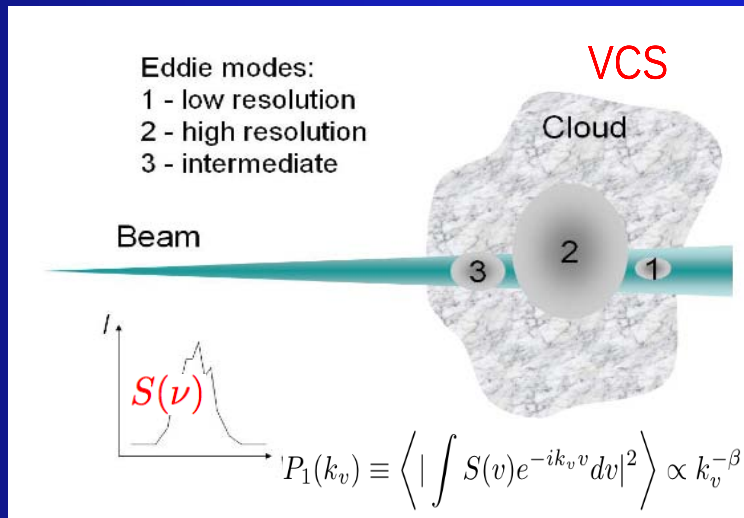

Developed in Lazarian & Pogosyan 06, 08

VCA and VCS techniques (Lazarian & Pogosyan 00, 04, 06, 08) reveal turbulence velocity spectra in agreement with expectations for supersonic turbulence

Expectations for supersonic turbulence

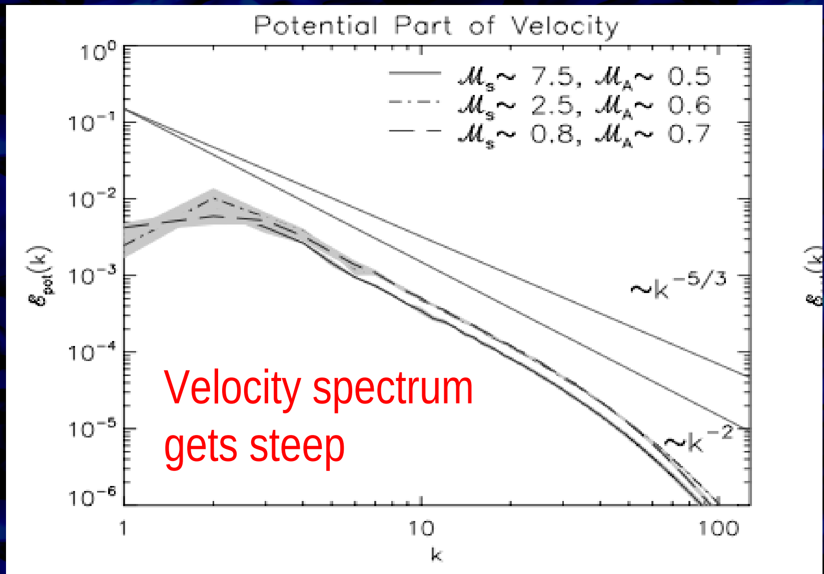

Kowal & Lazarian 2010

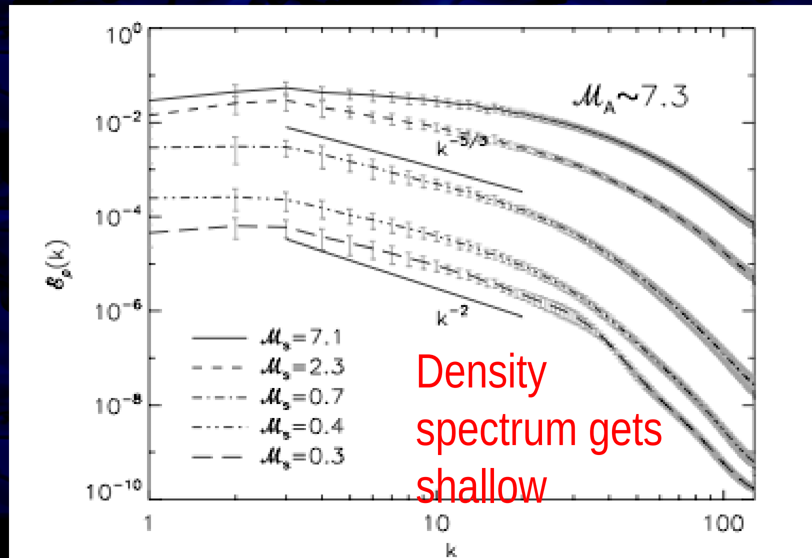

Kowal, Lazarian & Beresnyak 2007

Selec

VCS gets

for high latitude galactic HI $E_v \sim k^{-1.87}$ (Chepurnov et al.08,10)

for ^{13}CO for the NGC 1333 $E_v \sim k^{1.85}$ (Padoan et al. 09)

indicating supersonic turbulence. Density is shallow $\sim k^{-08}$

Dynamics of magnetic fields is essential, but whether the picture is self-consistent

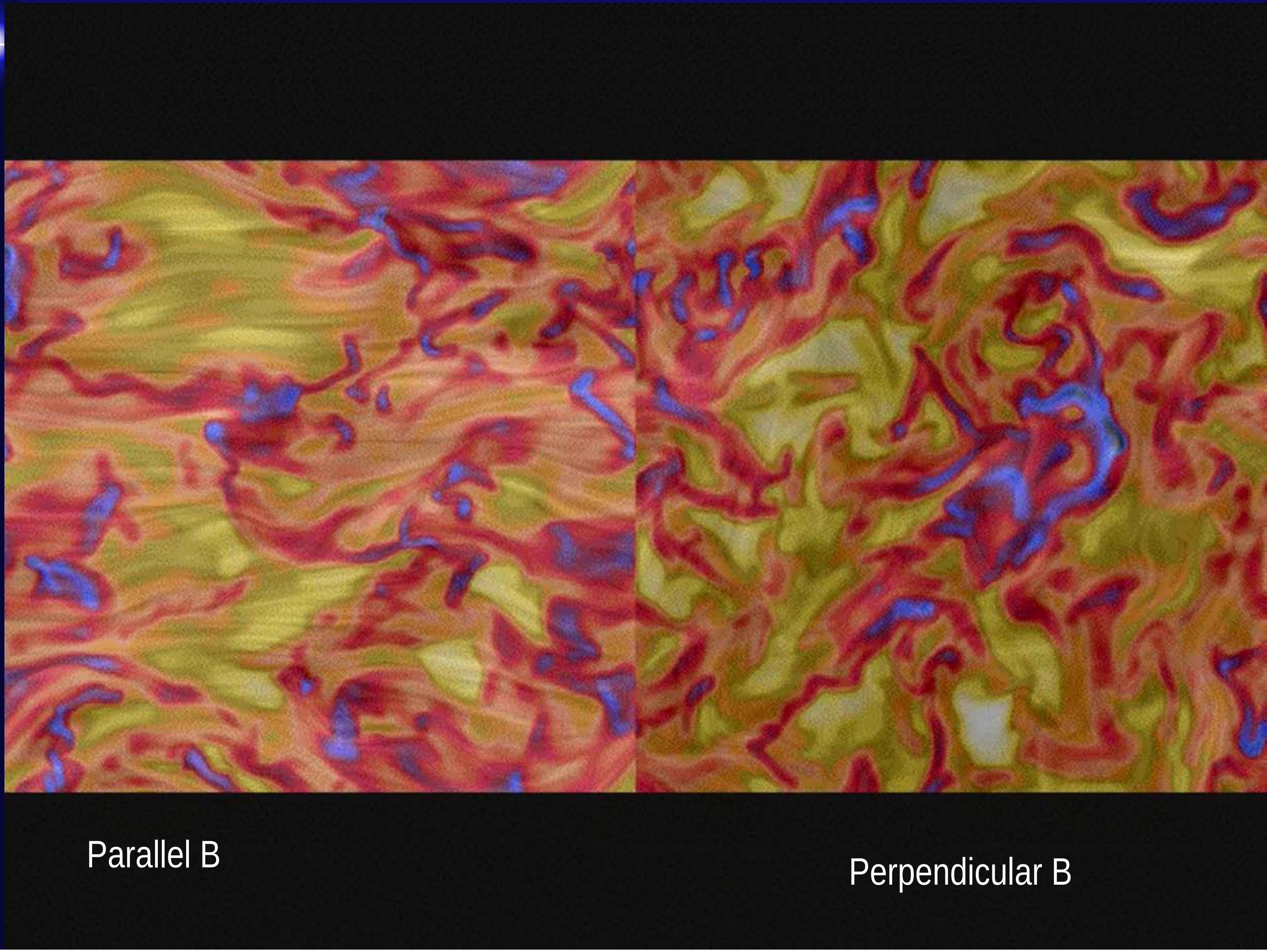

512^3

Part II. What does magnetic field do in turbulent fluid?

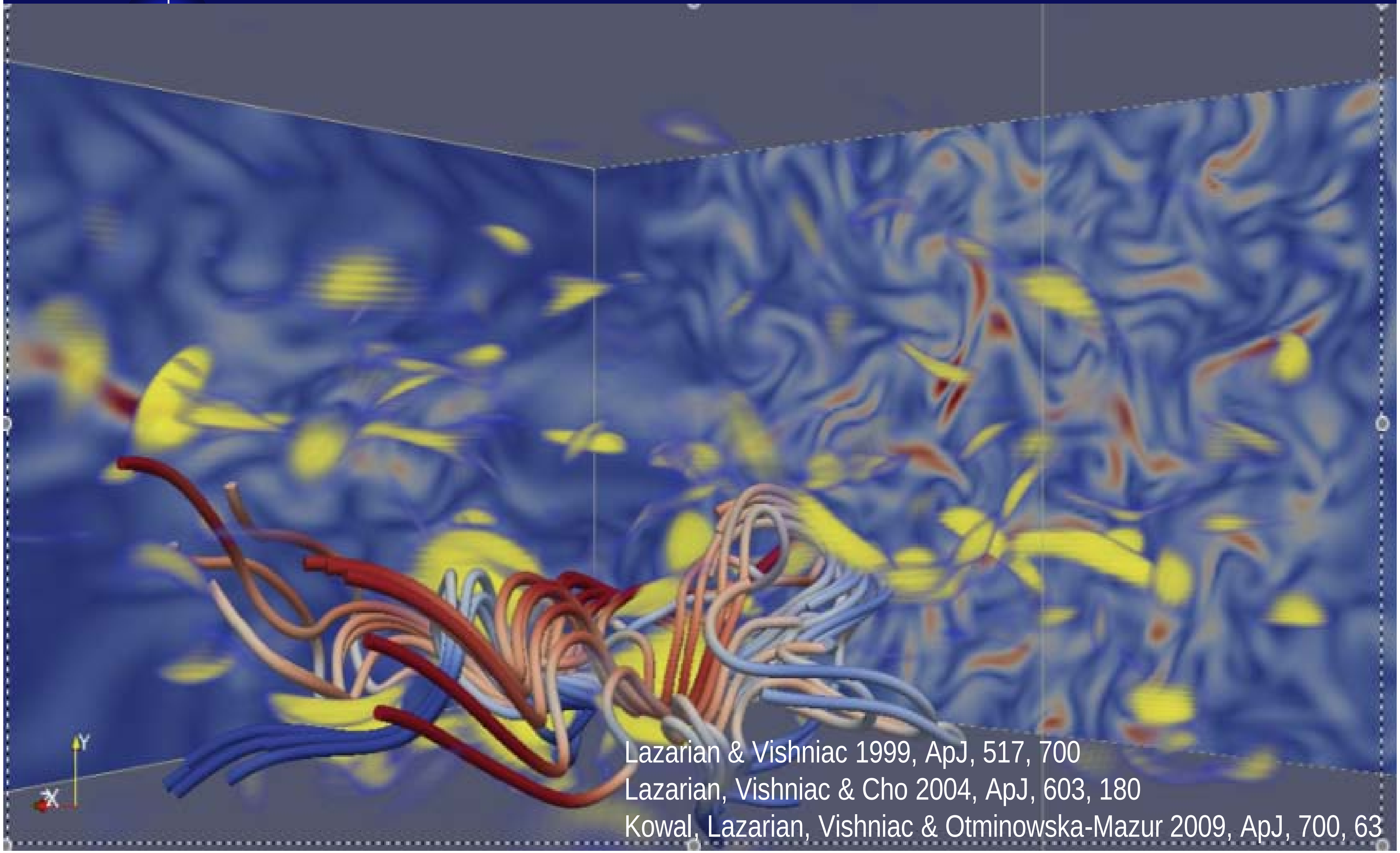

Classical Sweet-Parker model very slow speed ~ 10^{-6} V_A for ISM

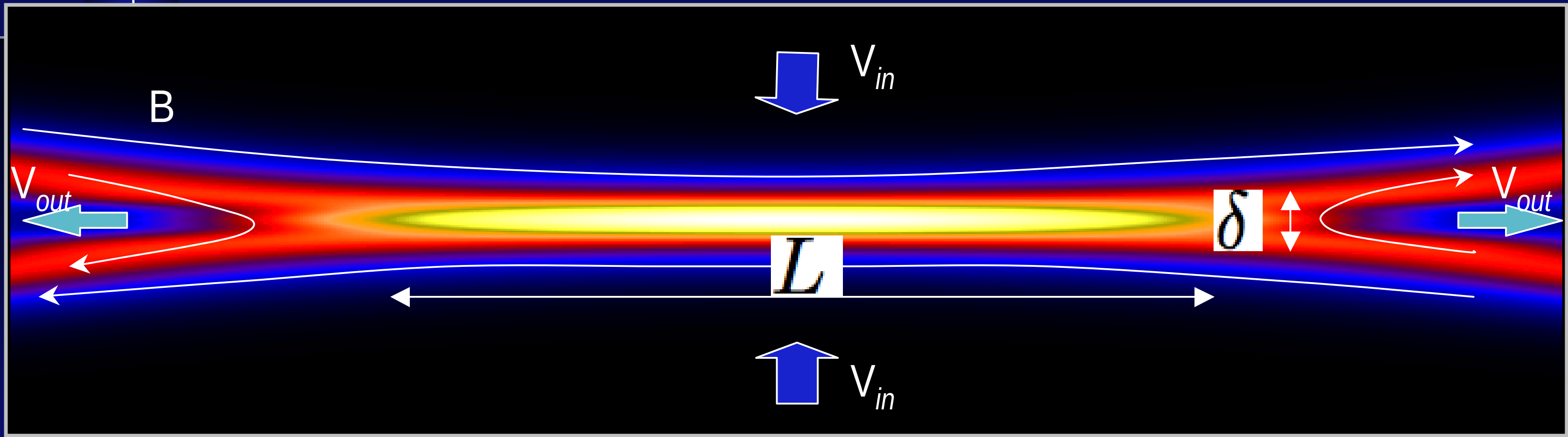

$$V_{in} = \eta/\delta$$ Ohmic diffusion

$$V_{in} L = V_{out} \delta$$ Mass conservation

$$V_{out} = V_A$$ Free outflow

RECONNECTION RATE

$$V_{in} = V_A (L V_A/\eta)^{-1/2} = V_A Rm^{-1/2}$$

For ISM $Rm>10^{12}$.

Petschek model does not work for uniform resistivities

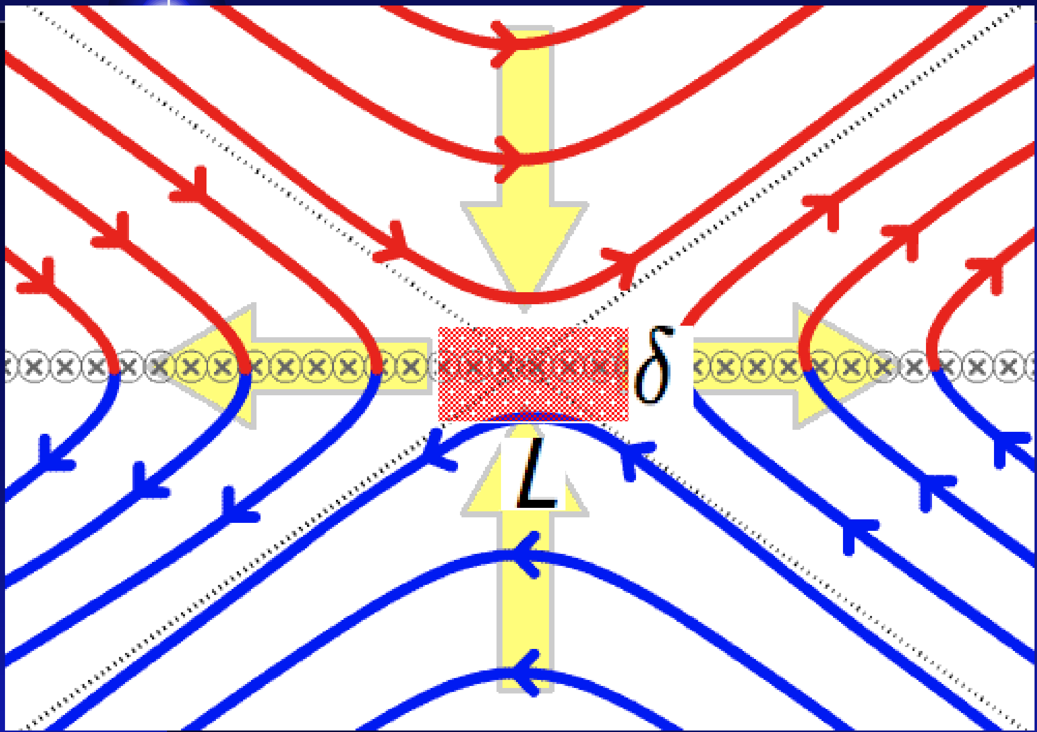

X point

Both dimensions are comparable.

$$L \sim \delta$$

Fast reconnection $V_R \sim V_A$

Fast collisionless Hall reconnection is not applicable to diffuse ISM and molecular clouds

o Petschek 1964 model of fast reconnection

ion current

e current

Very stringent requirement: mean free path of an electron is ~ L. If this is the necessary condition, all ISM simulations have no meaning.

Turbulence was discussed in terms of reconnection, but results were inconclusive

Microturbulence affects the effective resistivity by inducing anomalous effect

Some papers which attempted to go beyond this:

Speizer (1970) --- effect of line stochasticity in collisionless plasmas
Jacobs & Moses (1984) --- inclusion of electron diffusion perpendicular mean B
Strauss (1985), Bhattacharjee & Hameiri (1986) --- hyperresistivity
Matthaeus & Lamkin (1985) --- numerical studies of 2D turbulent reconnection

Kim & Diamond (2001) found constraints on the effects of turbulence on reconnection for 2.5 flows.

Reconnection of 3D weakly turbulent magnetic fields involves many simultaneous reconnection events

Turbulent reconnection:

1. Outflow is determined by field wandering.

2. Reconnection is fast with Ohmic resistivity only.

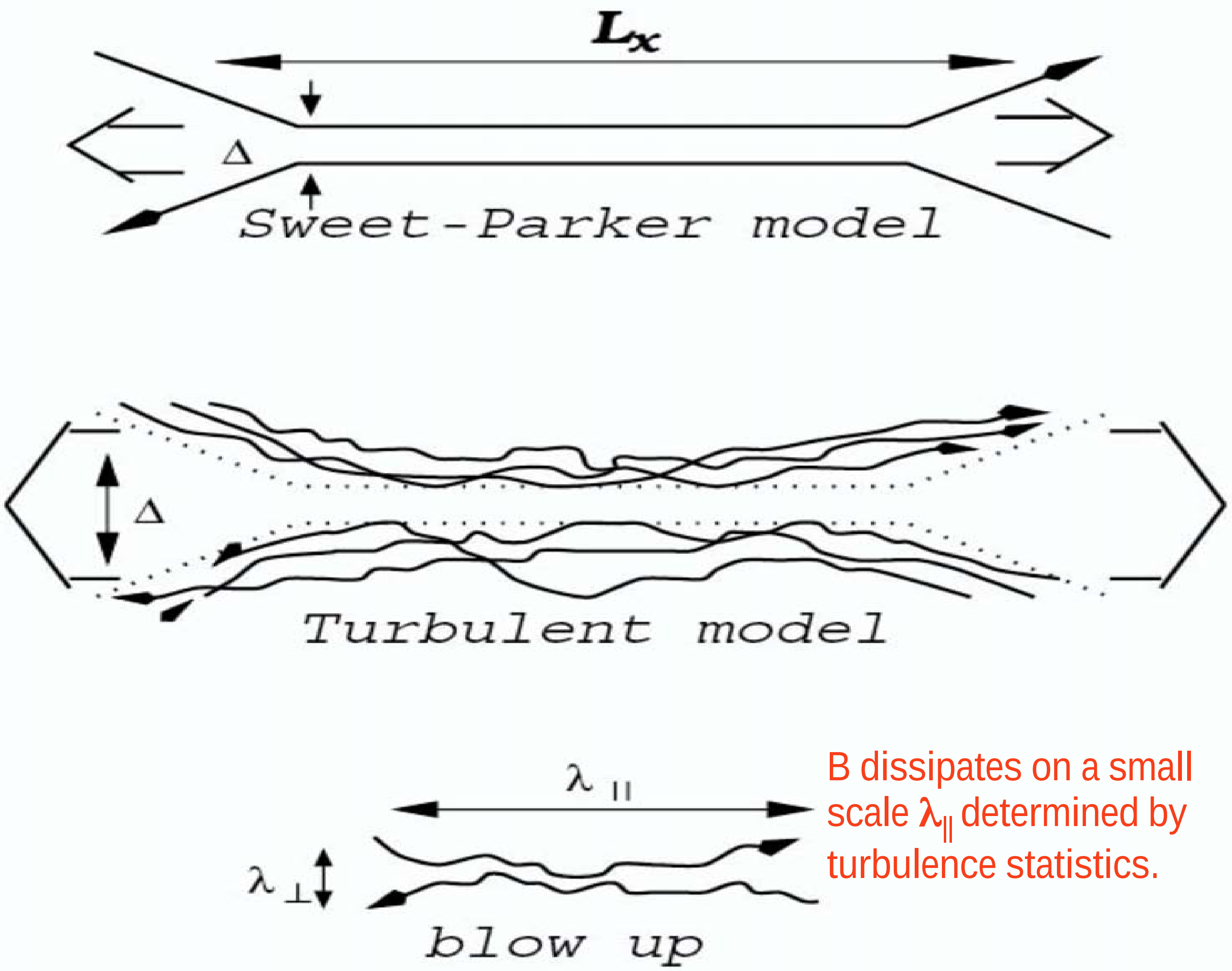

B dissipates on a small scale $\lambda_{\parallel}$ determined by turbulence statistics.

Key element:

$L/\lambda_{\parallel}$ reconnection simultaneous events

Lazarian & Vishniac (1999)

henceforth referred to as LV99

Bottle neck is the outflow width: field wandering determines the reconnection rate

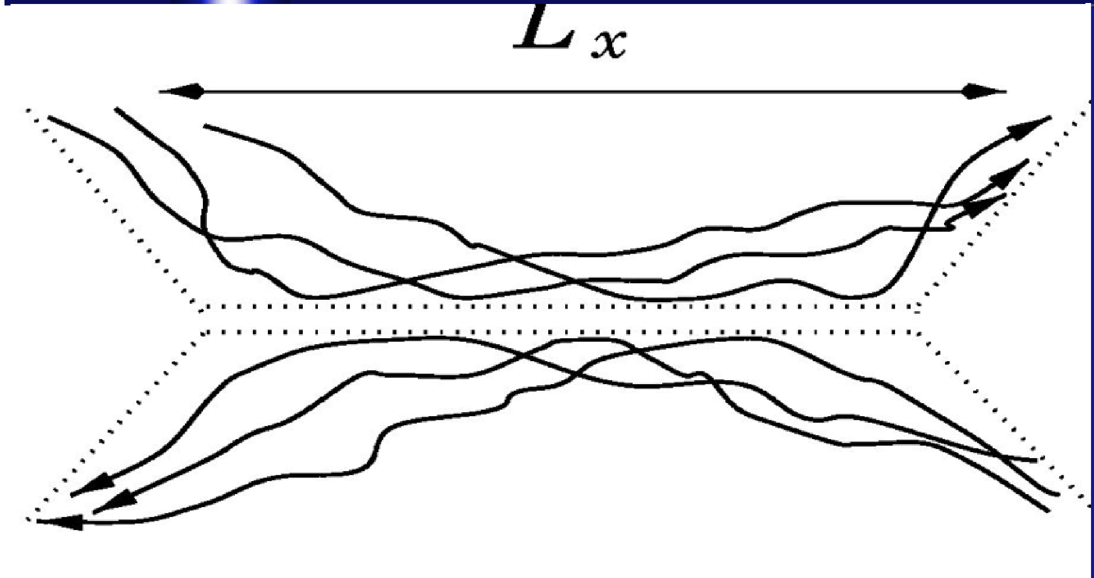

Predictions in Lazarian & Vishniac (1999):

No dependence on anomalous or Ohmic resistivities!

$$V_{rec} = V_A \left(\frac{l_{inj}}{L_x}\right)^{1/2} \left(\frac{v_{inj}}{V_A}\right)^2$$

As $P_{inj} \sim v_{inj}^4/(lV_A)$ it translates into $V_{rec} \sim l_{inj} P_{inj}^{1/2}$

Within the last decade a substantial convergence between the models took place

Hall MHD 1999

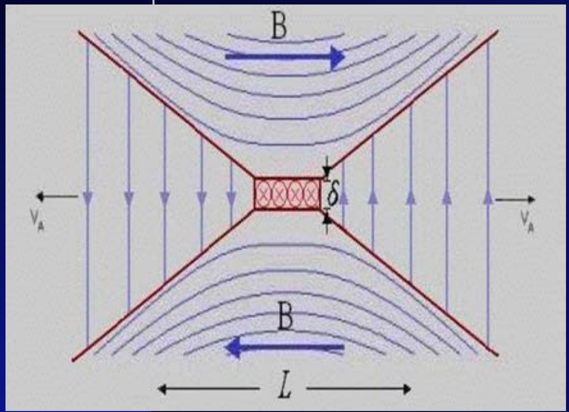

Our model

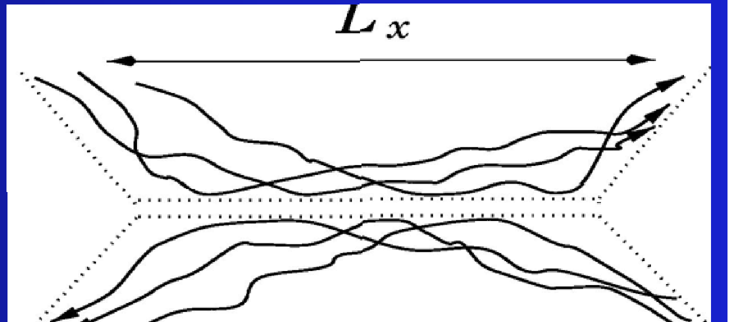

Lazarian & Vishniac 1999

Hall MHD 2009

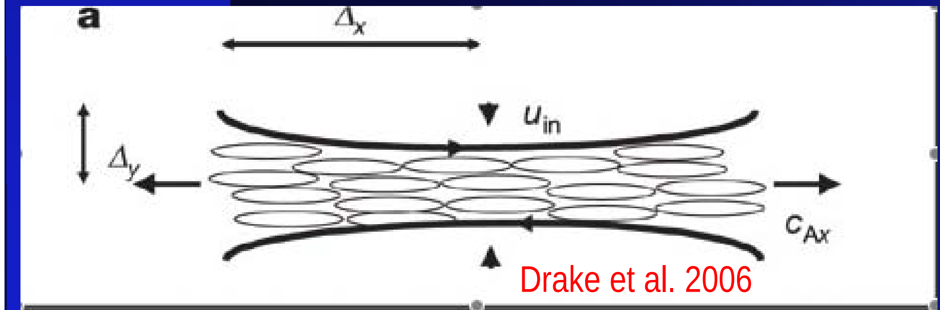

Drake et al. 2006

Our model is the one of volume filled reconnection. John Raymond attempted to test our model, confirmed its predictions, but by that time the Hall MHD model evolved…

All calculations are 3D with non-zero guide field

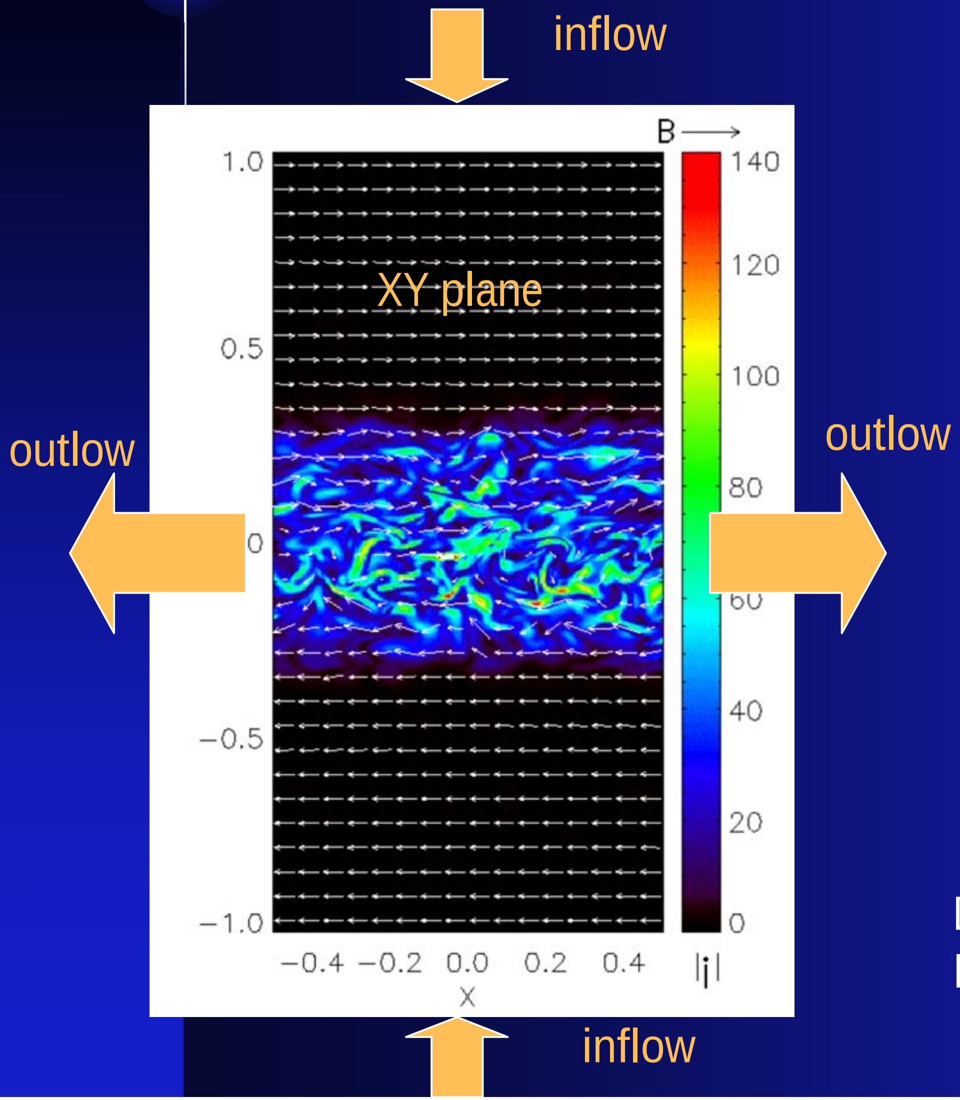

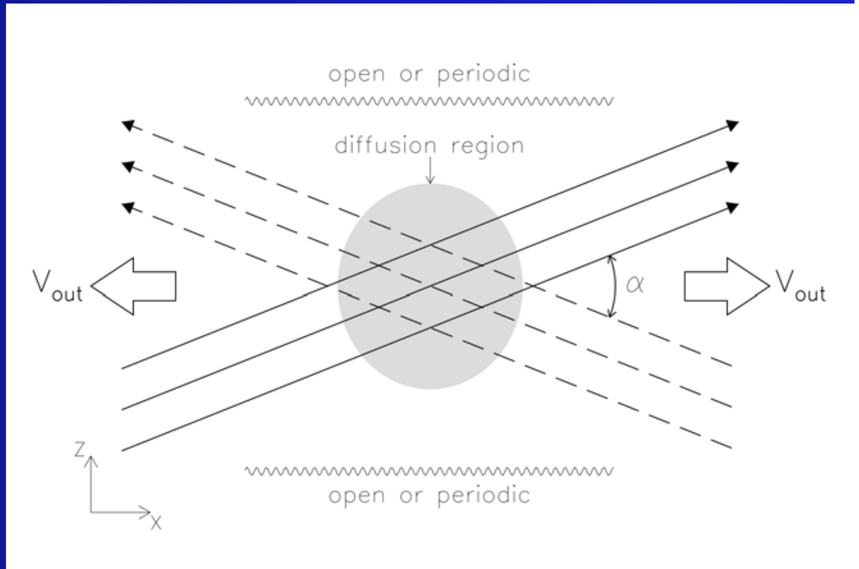

Magnetic fluxes intersect at an angle

Driving of turbulence: r_d=0.4, h_d=0.4 in box units.
Inflow is not driven.

We solve MHD equations with outflow boundaries

MHD equations with turbulence forcing:

$$\frac{\partial \rho}{\partial t} + \nabla \cdot (\rho \vec{v}) = 0$$

$$\frac{\partial \rho \vec{v}}{\partial t} + \nabla \cdot \left[\rho \vec{v} \vec{v} + \left(c_s^2 \rho + \frac{B^2}{8\pi} \right) \vec{I} - \frac{1}{4\pi} \vec{B} \vec{B} \right] = \rho \vec{f}$$

$$\frac{\partial \vec{B}}{\partial t} = \nabla \times \left(\vec{v} \times \vec{B} + \eta \nabla \times \vec{B} \right), \nabla \cdot \vec{B} = 0$$

isothermal EOS

Forcing:

- random with adjustable injection scale (k_f~8 or 16)

- divergence free (purely incompressible forcing)

Resistivity:

-Ohmic

-Anomalous

Kowal, Lazarian, Vishniac & Otminowska-Mazur (2009) ApJ 700, 63-85

We used both an intuitive measure, V_{inflow}, and a new measure of reconnection

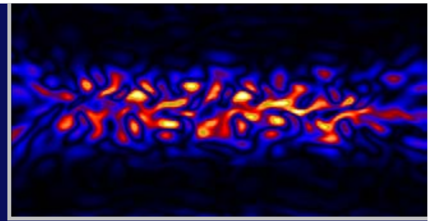

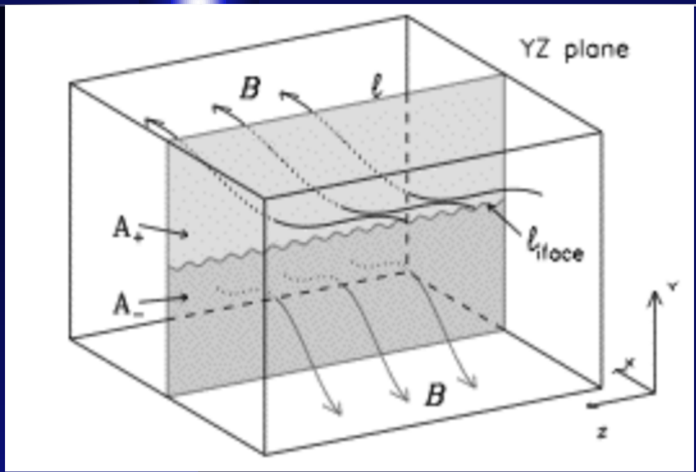

$$\partial_t \Phi = -\oint \boldsymbol{E} \cdot d\boldsymbol{l} = \oint (\boldsymbol{v} \times \boldsymbol{B} - \eta \boldsymbol{j}) \cdot d\boldsymbol{l}$$

$$\partial_t \Phi_+ - \partial_t \Phi_- = \partial_t \int |B_x| dA,$$

$$\partial_t \int |B_x| dS = \oint \vec{E} \cdot d\vec{l}_+ - \oint \vec{E} \cdot d\vec{l}_- = \oint sign(B_x) \vec{E} \cdot d\vec{l} + \int 2\vec{E} \cdot d\vec{l}_{interface}$$

$$\int 2\vec{E} \cdot d\vec{l}_{interface} \equiv -2 V_{rec} |B_{x,\infty}| L_z$$

Asymptotic absolute value of Bx

New measure:

$$V_{rec} = -\frac{1}{2|B_{x,\infty}| L_z} \left[\partial_t \int |B_x| dA - \oint sign(B_x) \vec{E} \cdot d\vec{l} \right]$$

Calculations using the new measure are consistent with those using the intuitive one

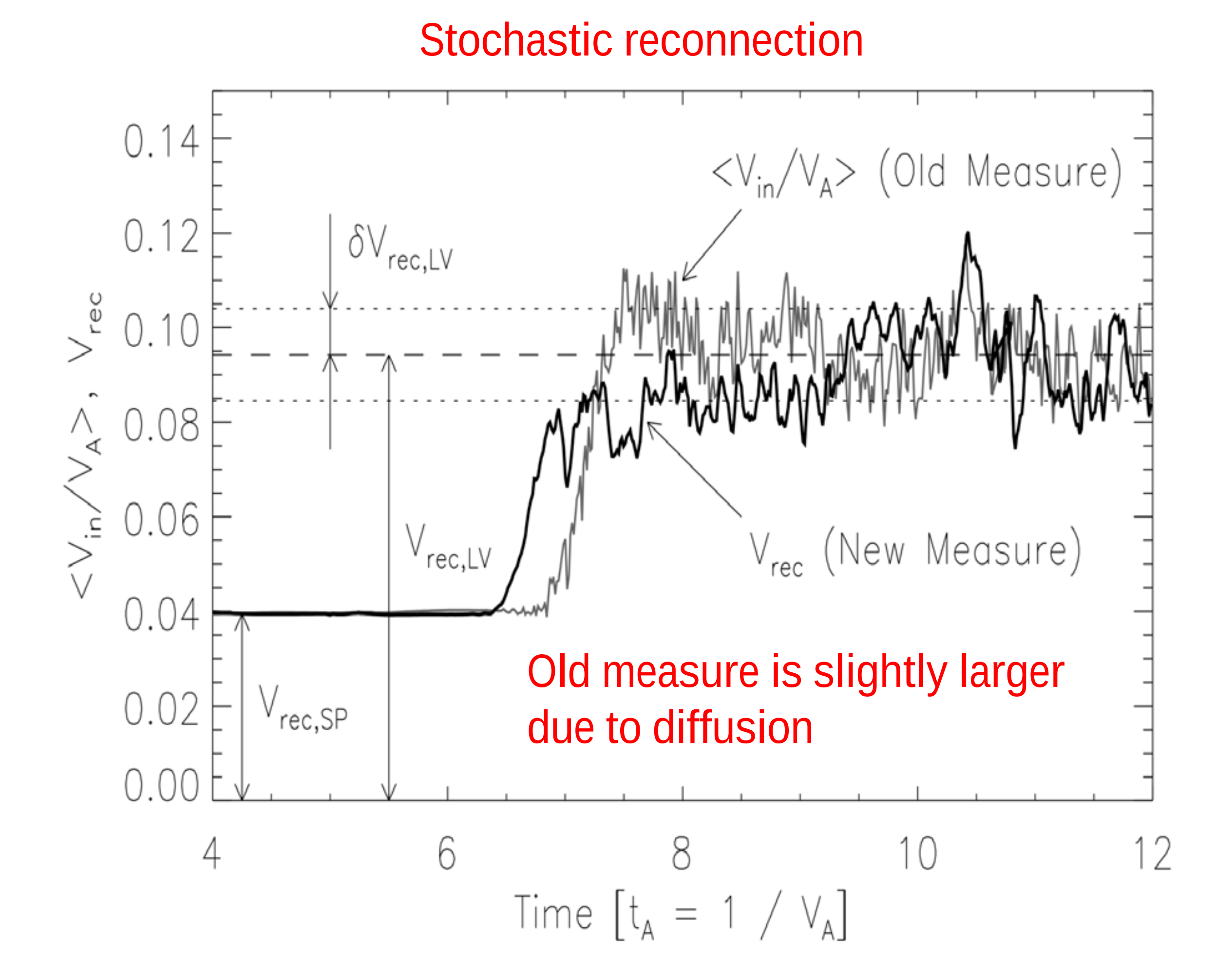

Intuitive, “old” measure is the measure of the influx of magnetic field

New measure probes the annihilation of the flux

Reconnection is Fast: speed does not depend on Ohmic resistivity!

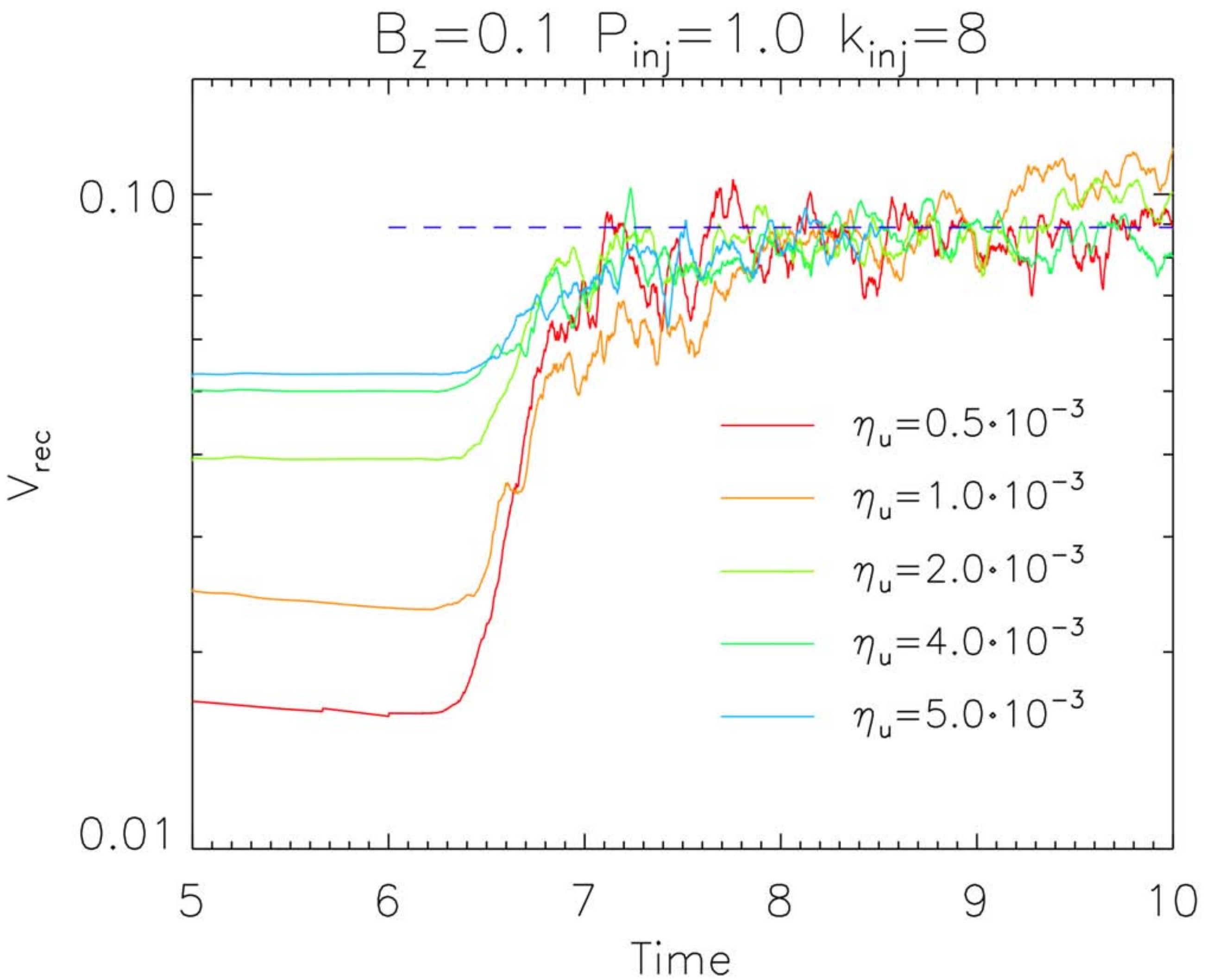

Lazarian & Vishniac 1999 predicts no dependence on resistivity

Results do not depend on the guide field

The reconnection rate increases with input power of turbulence

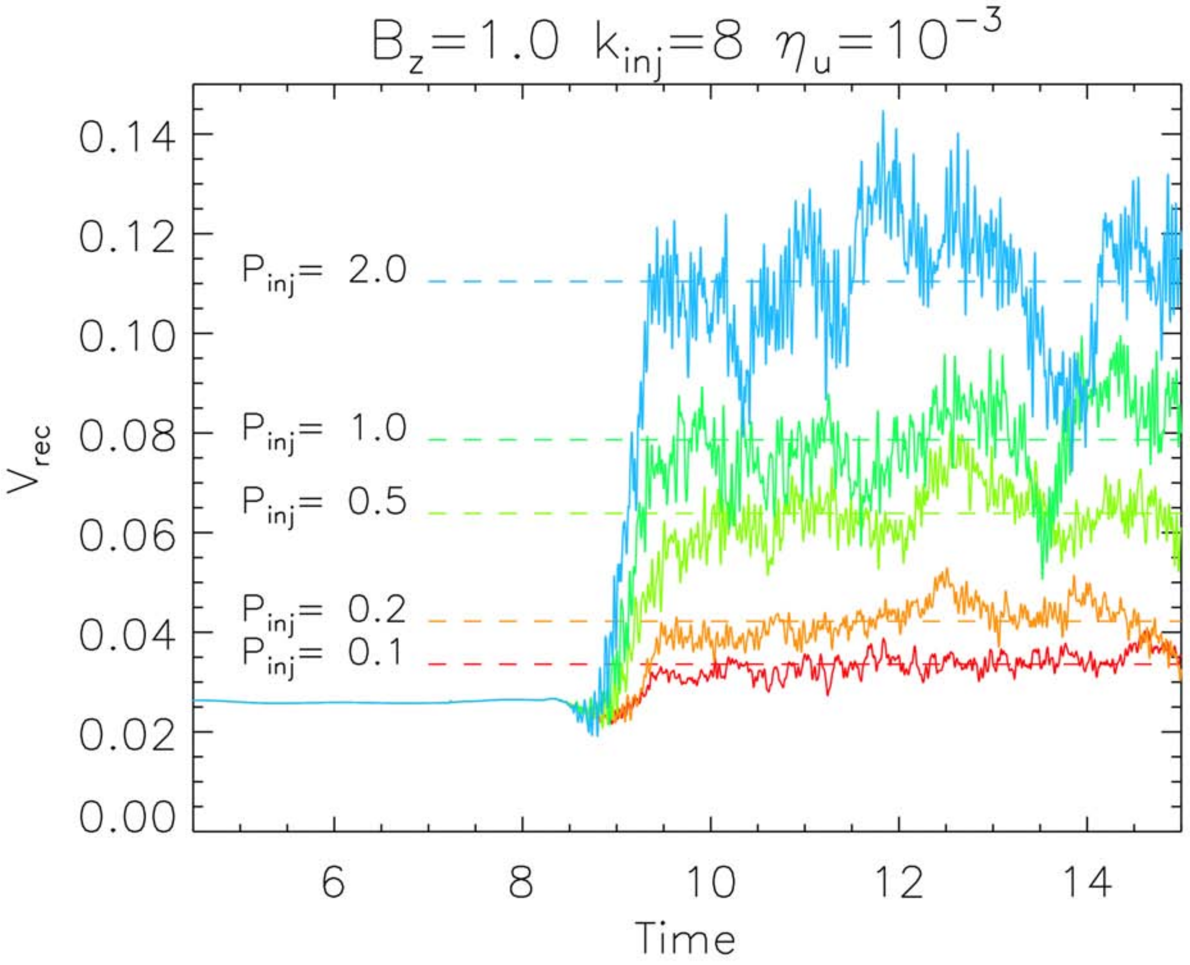

Lazarian & Vishniac (1999) prediction is $V_{rec} \sim P_{inj}^{1/2}$

Results do not depend on the guide field

Reconnection rate does not depend on anomalous resistivity

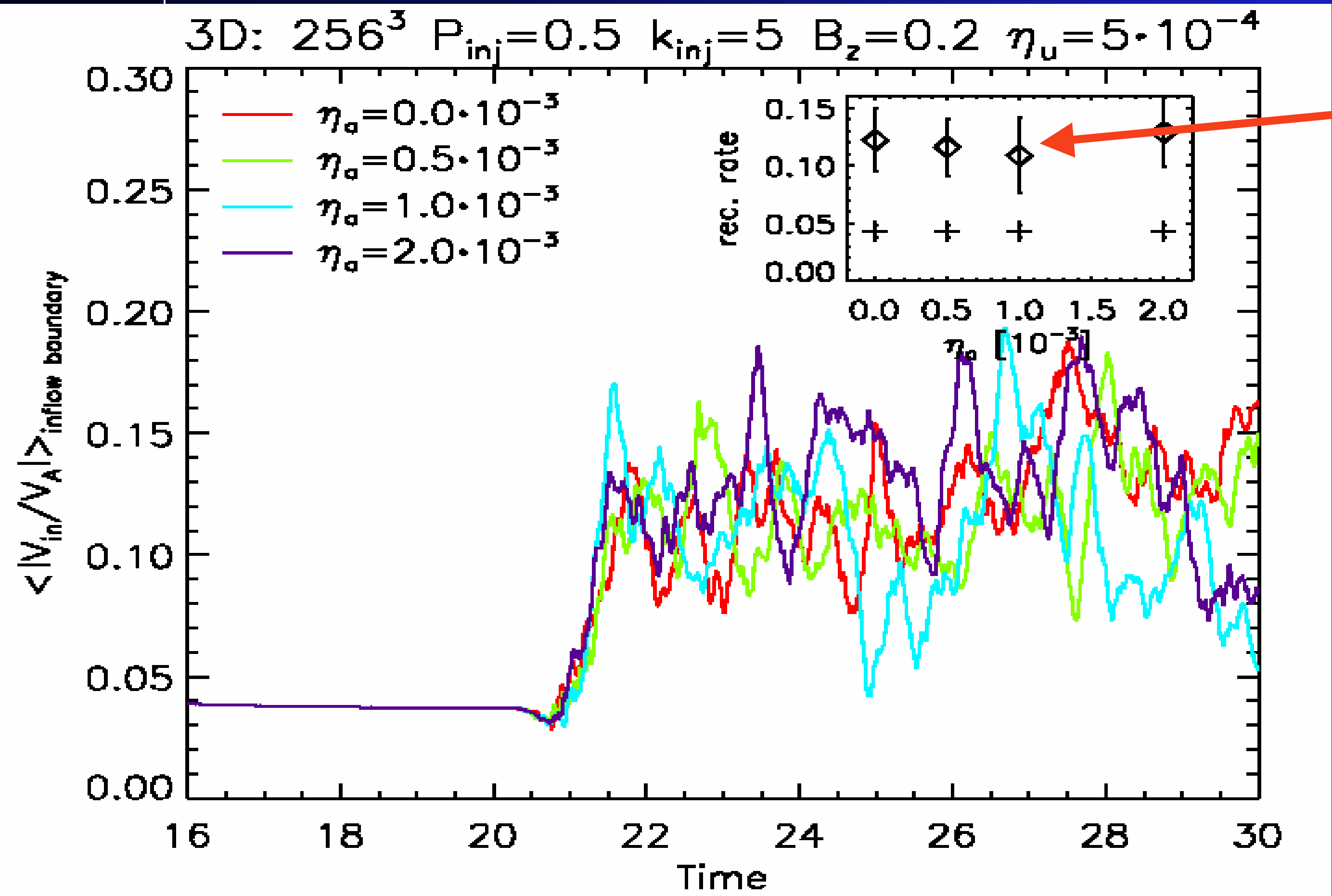

Flat dependence on anomalous resistivity

Reconnection does not require Hall MHD

LV99 model of reconnection gains support from Solar flare observations

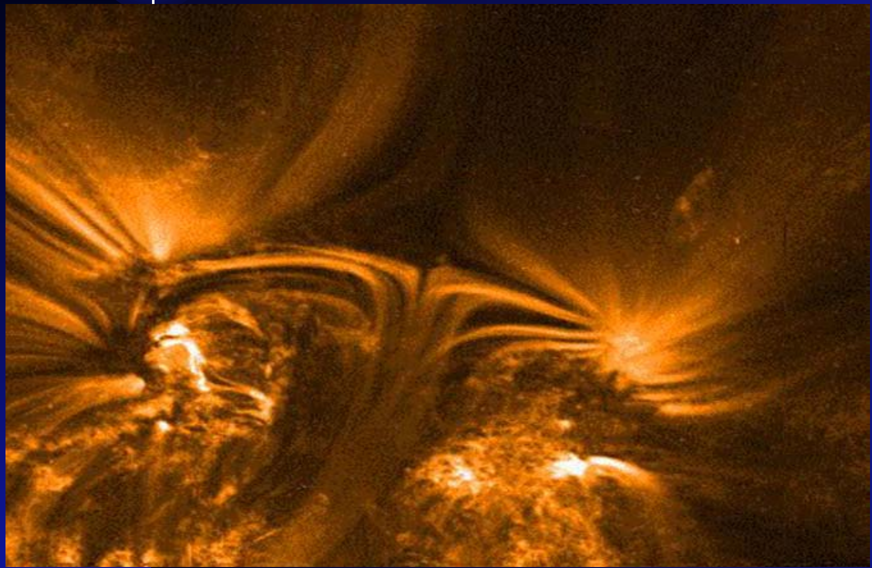

1. Solar flares can only be explained if magnetic reconnection can be initially slow (to accumulate flux) and then fast (to explain flares). Level of turbulence can do this (LV99)
2. Thick current layers predicted by LV99 have been observed in Solar flares (Ciaravella, & Raymond 2008).
3. Predicted by LV99 triggering of magnetic reconnection by Alfven waves was observed by Sych et al. (2009).

Indirect support for the LV99 model comes from different sources

1. Acceleration of anomalous cosmic rays (Lazarian & Opher 2009).
2. Cosmic ray anisotropies observed by MILAGRO and ICECUBE (Lazarian & Desiati 2010).
3. Absence of the correlation of density and magnetic field in diffuse ISM (Lazarian 2005).
4. Fast removal of magnetic fields observed in protostellar cores (Santos de Lima et al. 2010).
5. Differences of magnetization of cloud cores and ambient media (Crutcher et al. 2009).

In addition, the LV99 model corresponds well to the ideas of spontaneous stochasticity that will be discussed tomorrow by G. Eyink

In our reconnection model energetic particles get accelerated by First Order Fermi mechanism

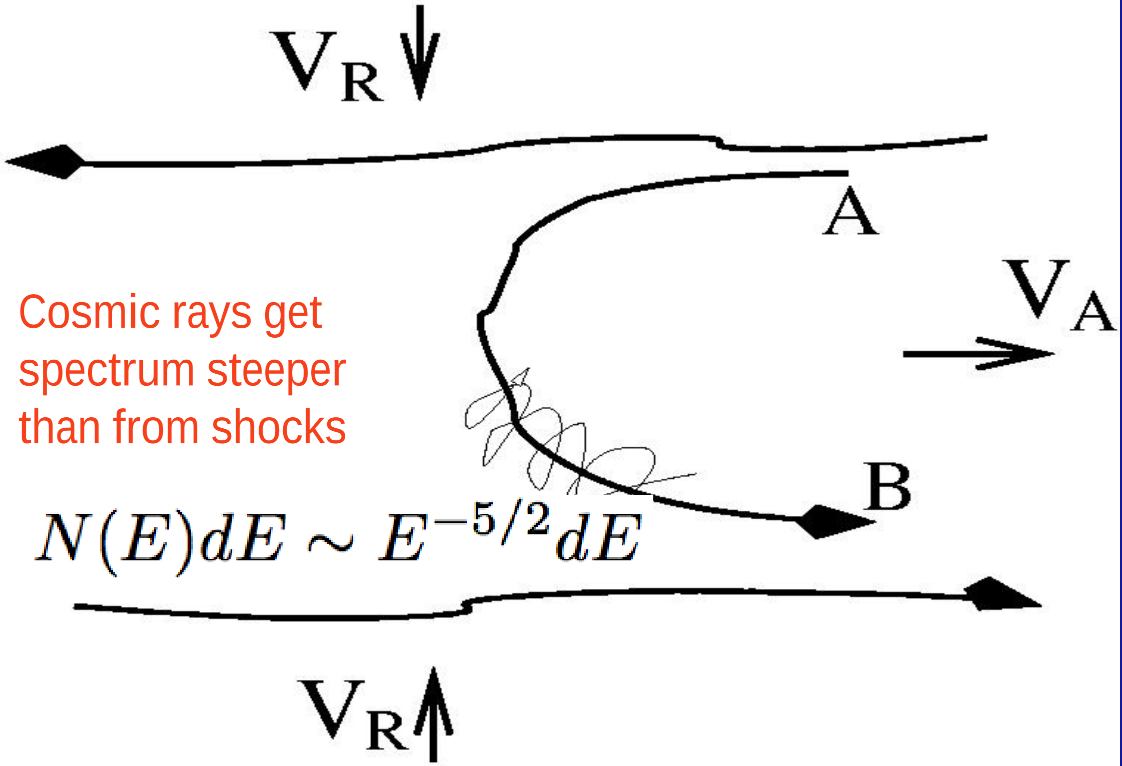

Cosmic rays get spectrum steeper than from shocks

$$N(E)dE \sim E^{-5/2}dE$$

(cp. Drake 2006).

De Gouveia Dal Pino & Lazarian 2003

Applications to pulsars, microquasars, solar flare acceleration (De Gouveia Dal Pino & Lazarian 00, 03, 05, Lazarian 05).

MHD calculations reproduce 2D PIC calculations by Drake et al and go beyond

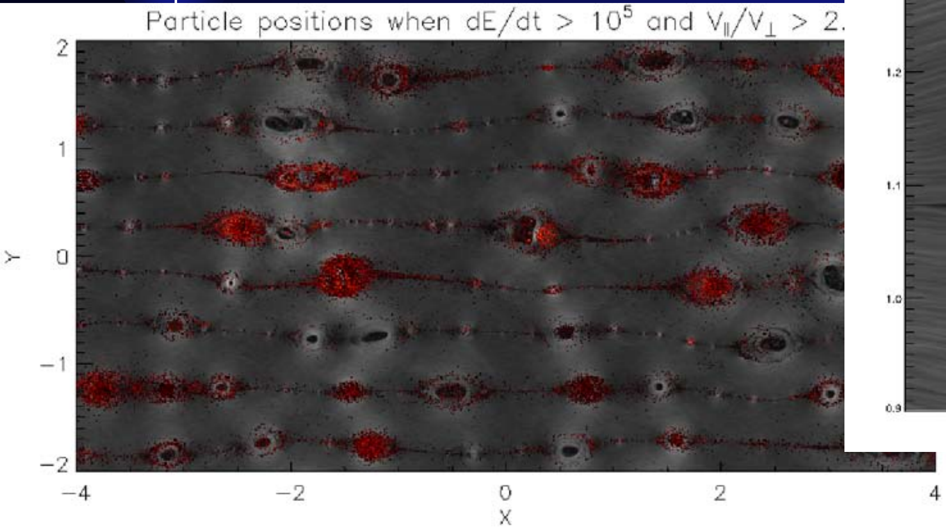

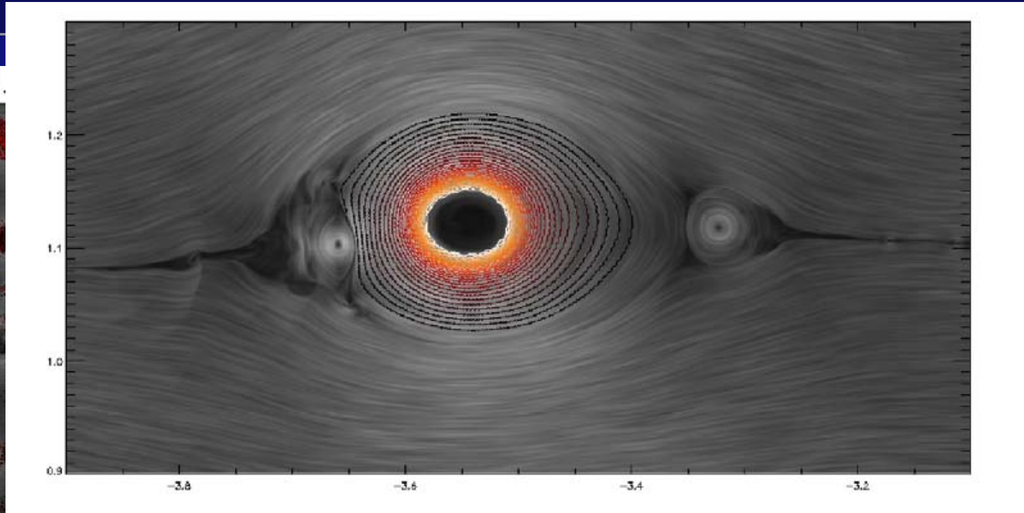

Zoom in into itrajectories

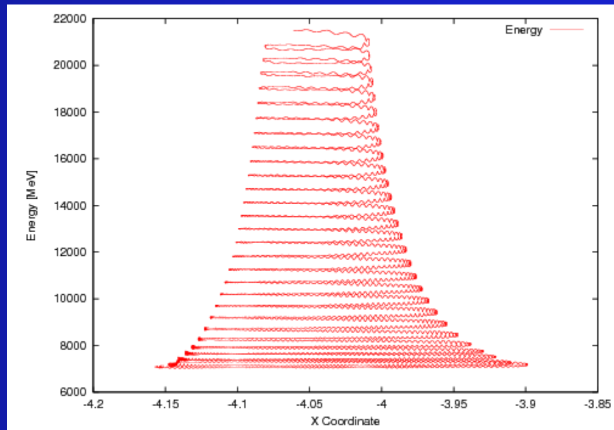

Regular energy increase

Multiple reconnection layers are used to produce volume reconnection.

Kowal, Lazarian, de Gouveial dal Pino 2011

Reconnection can provide a solution to anomalous cosmic ray measurements by Voyagers

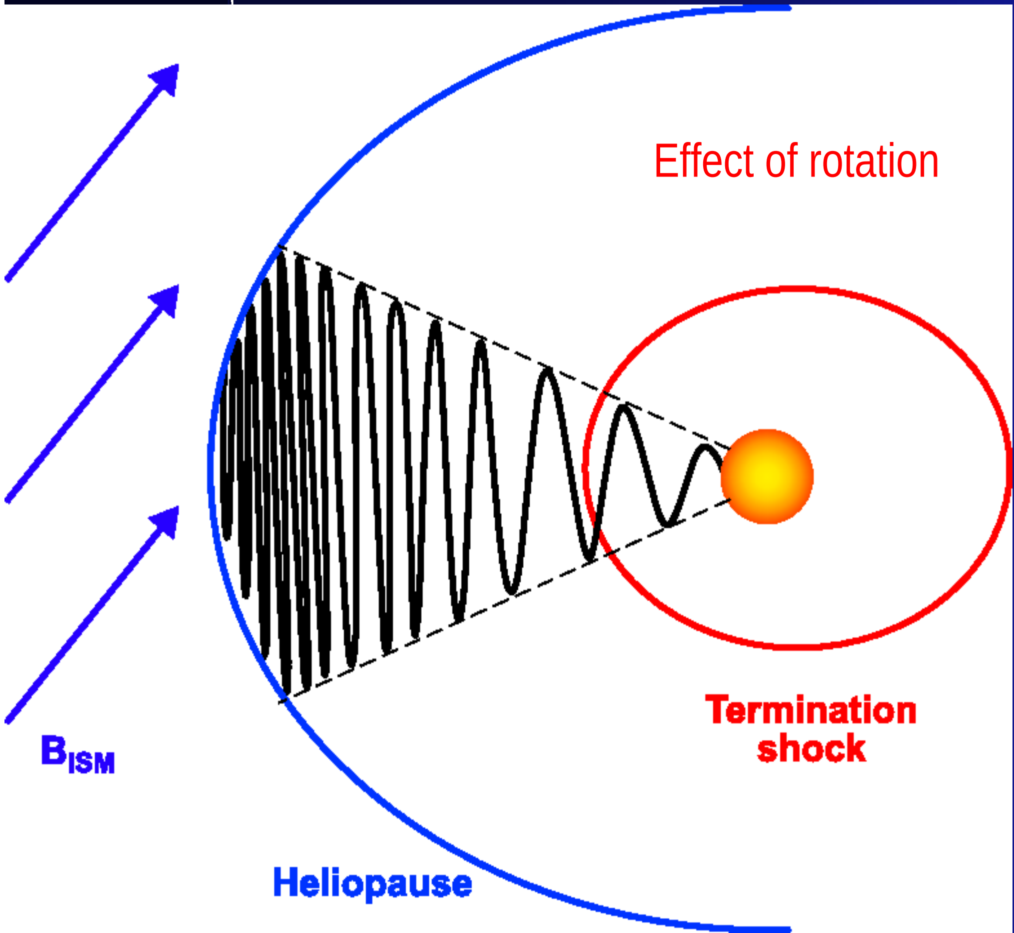

Observed anomalous CRs do not show features expected from the acceleration in the termination shock

Lazarian & Opher 2009: Sun rotation creates B-reversals in the heliosheath inducing acceleration via reconnection
See also Drake et al. (2010.

MILAGRO data: Magnetic reconnection expected in magnetotail can explain both the TeV and lower energy excess observed

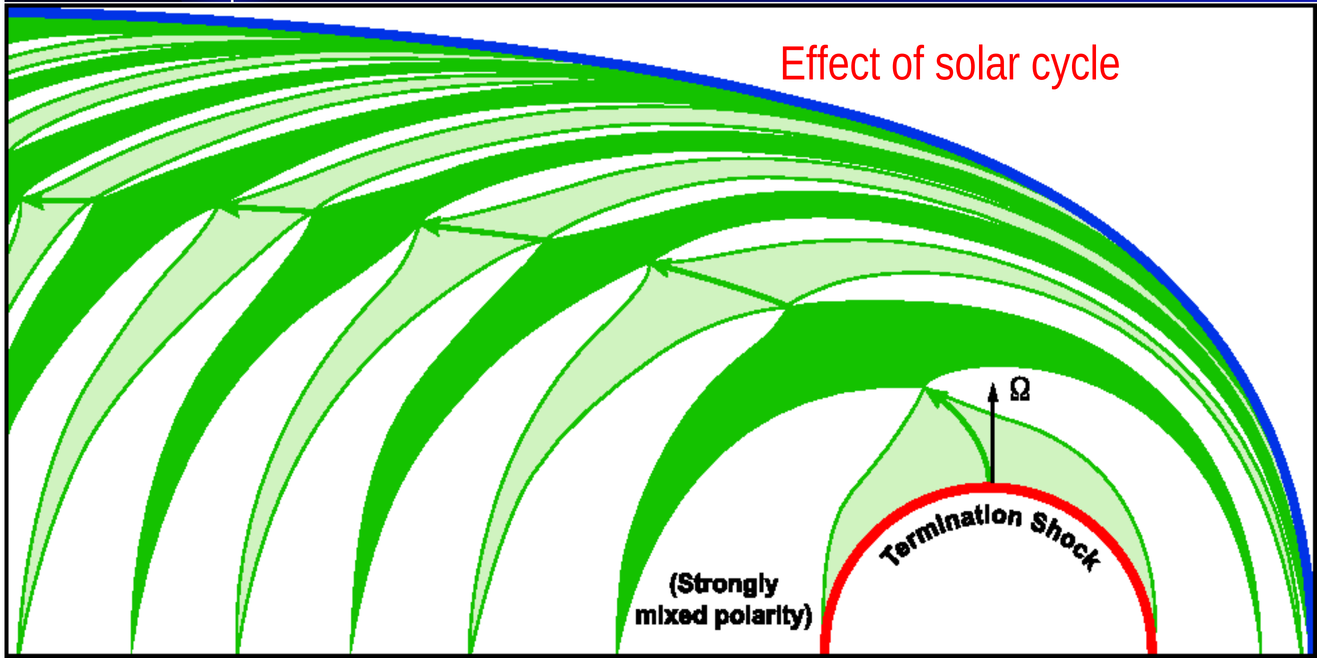

Lazarian & Desiatii 2010

$$E_{max} \approx 10^{13}\ \mathrm{eV} \left(\frac{B}{1\ \mu\mathrm{G}}\right) \left(\frac{L_{zone}}{2 \times 10^{15}\ cm}\right),$$

Simulations confirm predictions of LV99 model; this induces many astrophysical consequences to explore

Change in understanding of magnetic reconnection

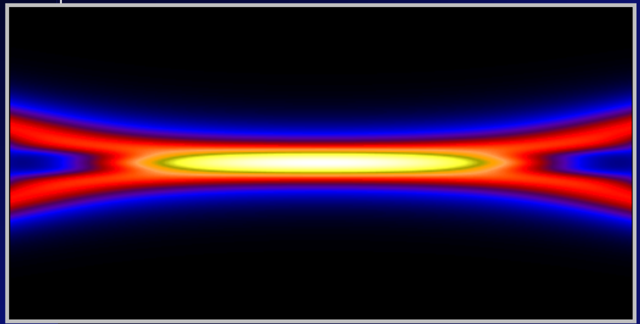

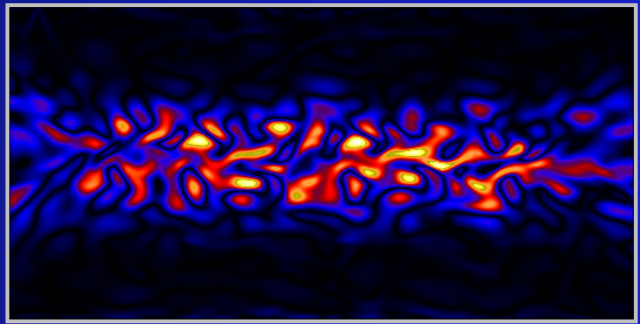

explains

Part III. Indirect evidence: acceleration in reconnection regions

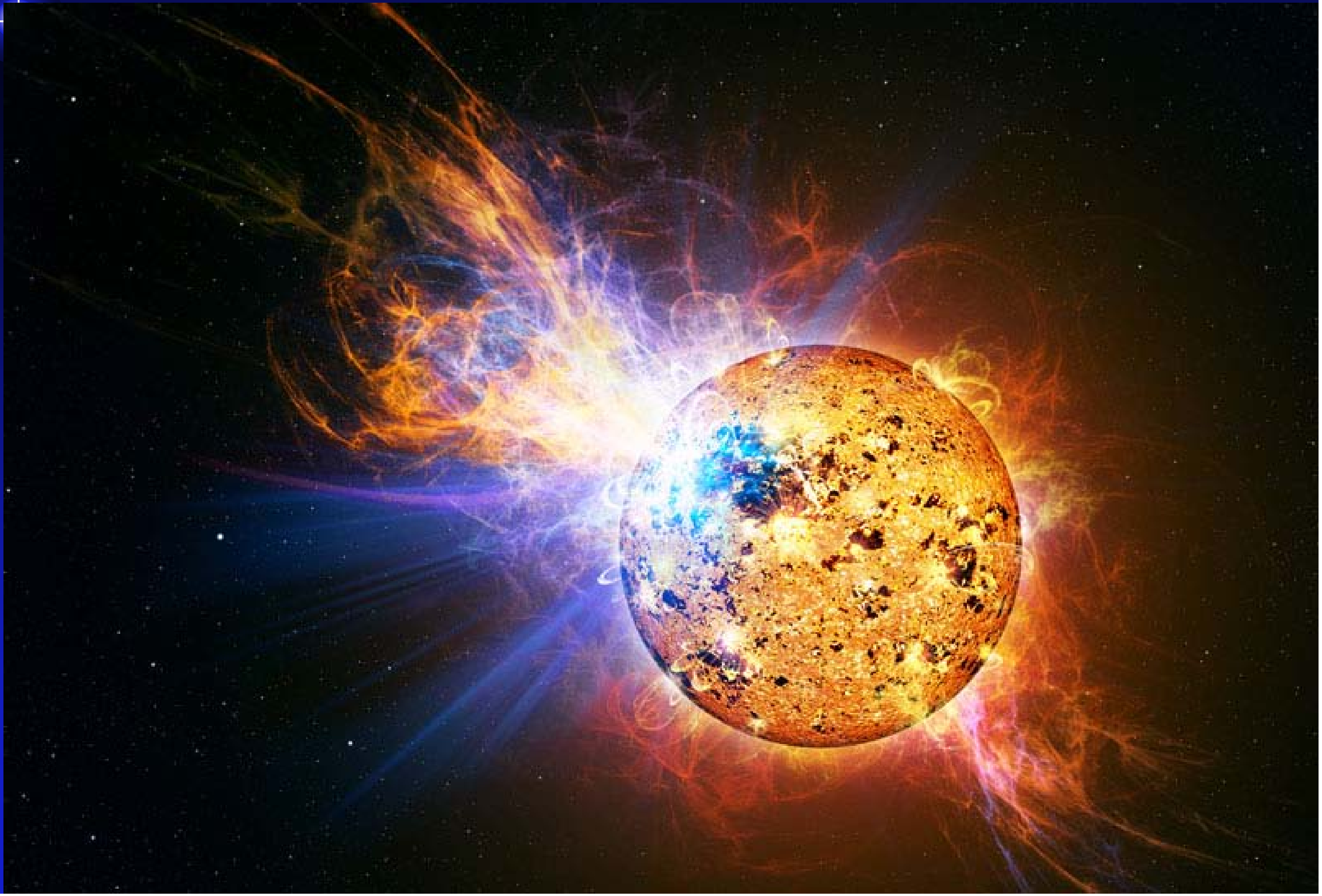

2D and 3D reconnection accelerates particles very differently: Loops and spirals behave differently!

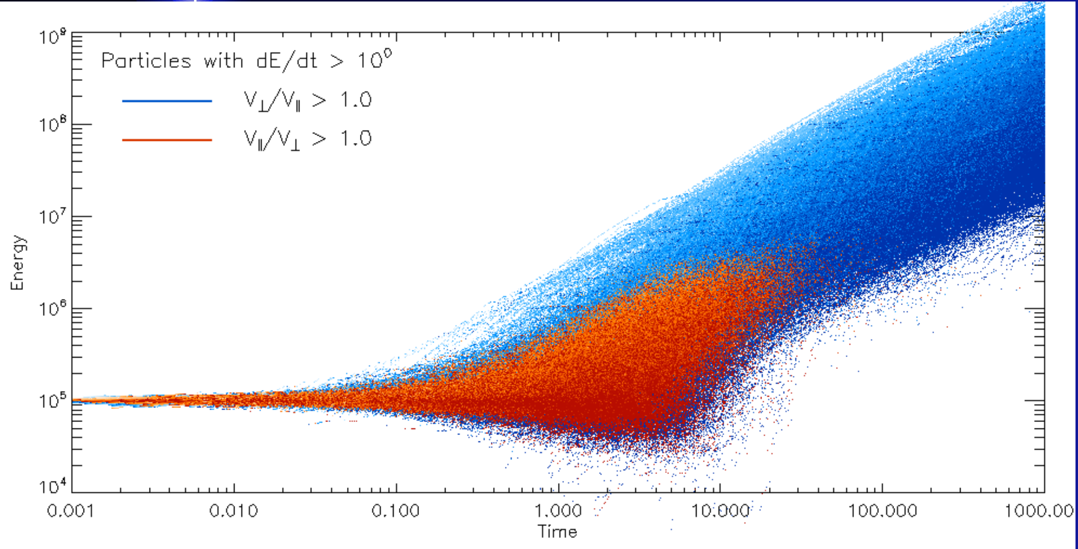

Perpendicular acceleration gets important for 2D at longer integration times

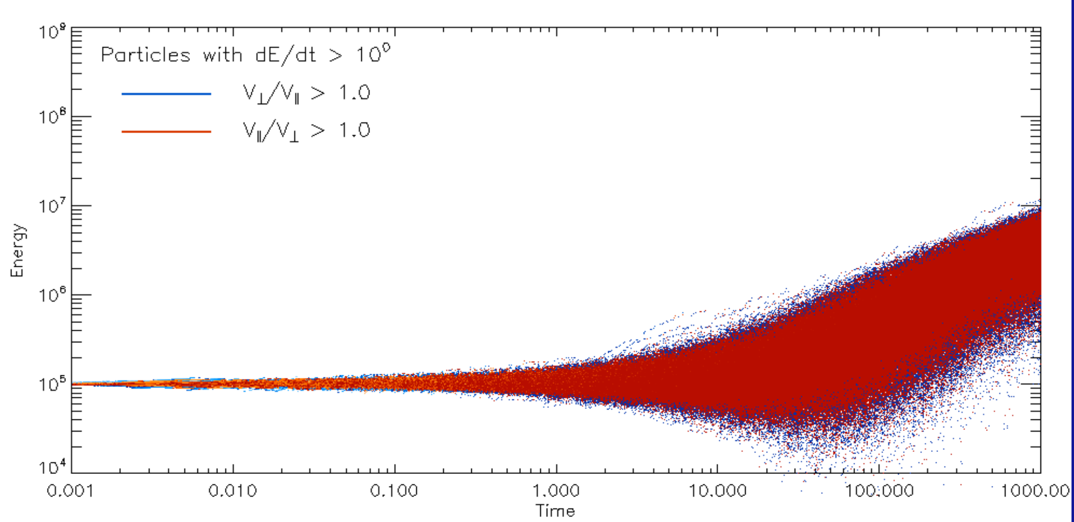

Parallel momentum mostly increases for the acceleration in 3D

Kowal, Lazarian, de Gouveial dal Pino 2010

MILAGRO data suggests the anisotropy of 5-10 TeV protons in the direction of magnetotail of the solar system

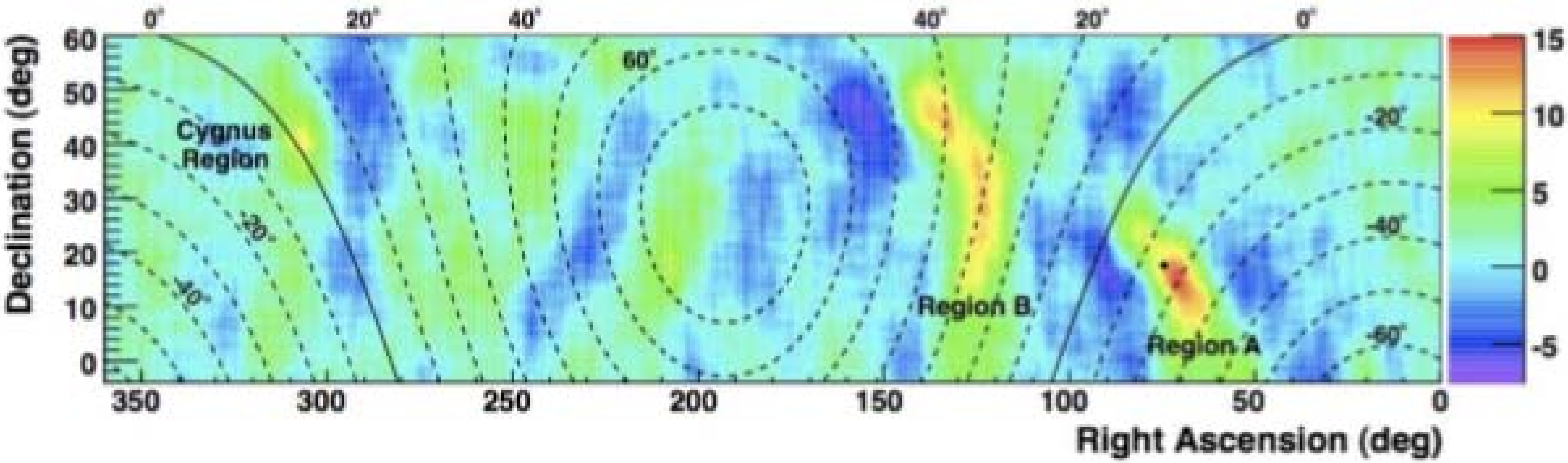

Attempted explanations include

1. the diffusion of CRs from the supernova explosion that created Geminga pulsar 340 000 years ago (Salvati & Sato 2008).
2. Free streaming of CRs in a magnetic bottle configuration (Drury & Aharonian 2009).
3. Propagation effects for CRs (Malkov et al. 2010).

Future Missions: Spectrum of Turbulence with Constellation X

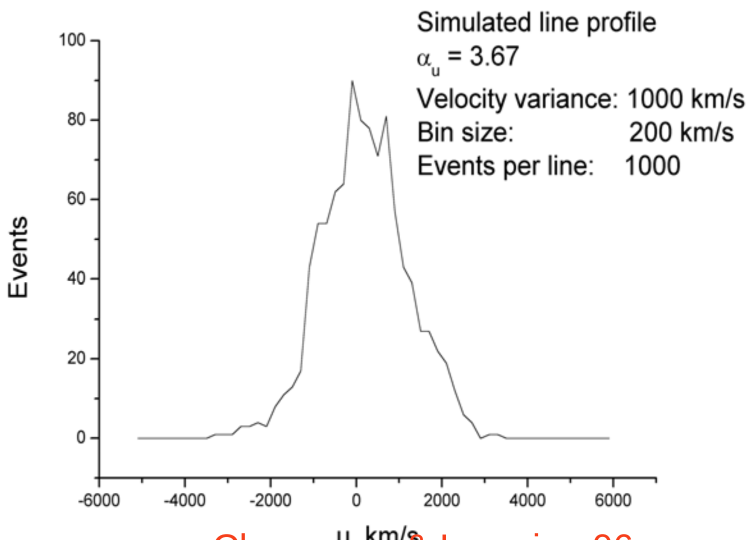

Chepurnov & Lazarian 06

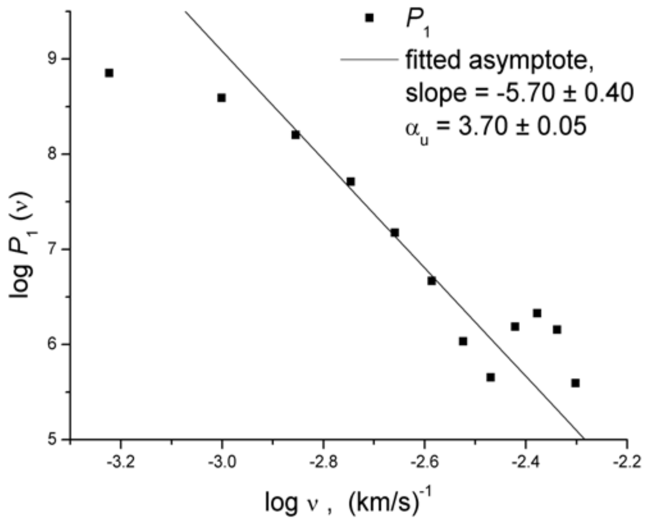

Studies of turbulence with new X-ray missions

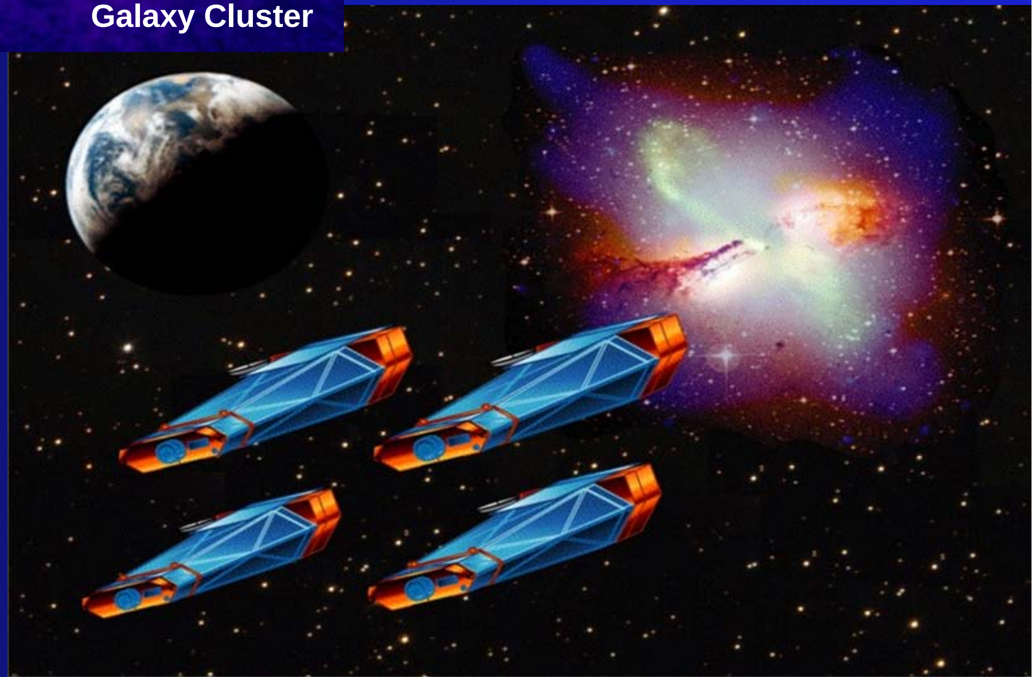

Constellation X will get turbulent spectra with VCS technique in 1 hour

VCS: Effect of Absorption

Absorption limits the range of scales that can be studied with VCS. The larger absorption, the smaller scales that can be studied.

Absorption Lines: Linear Regime

For absorption lines:

$$I_{\mathbf{X}}(v) = I_0 \exp[-\tau(\mathbf{X}, v)]$$

a new measure is appropriate

$$\langle [log(I(v_1) - logI(v_2)]^2 \rangle$$

The analysis is identical to LP00, but with logarithm of intensity instead of intensity

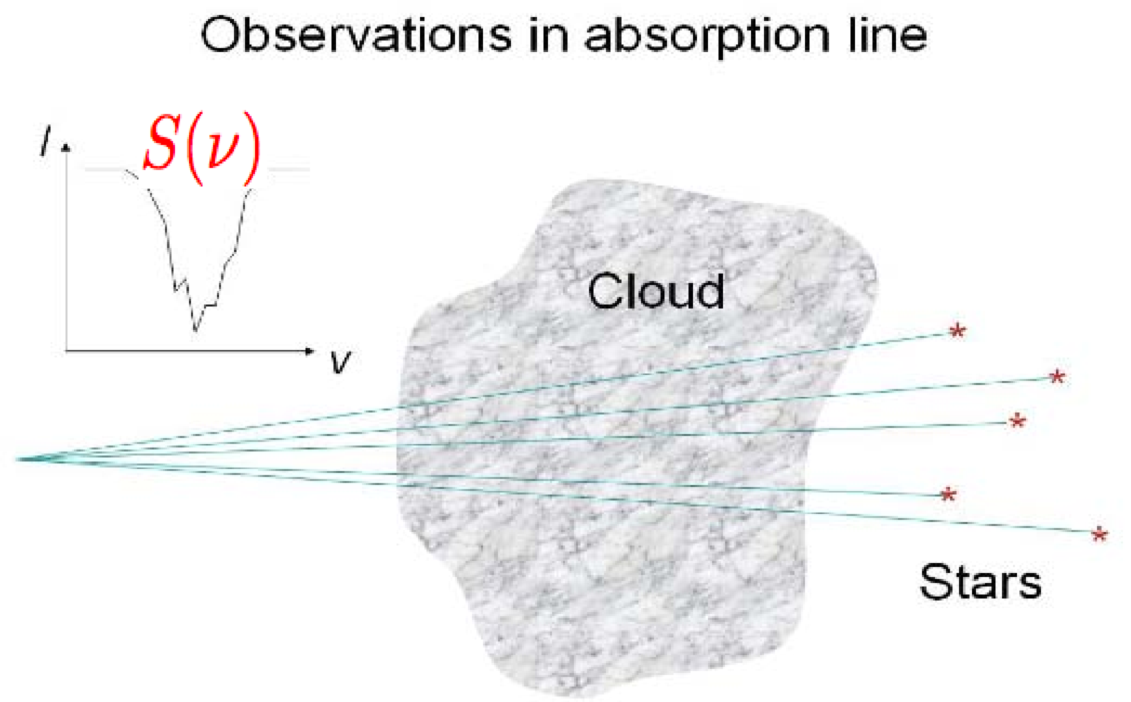

Number of Lines of Sight Required

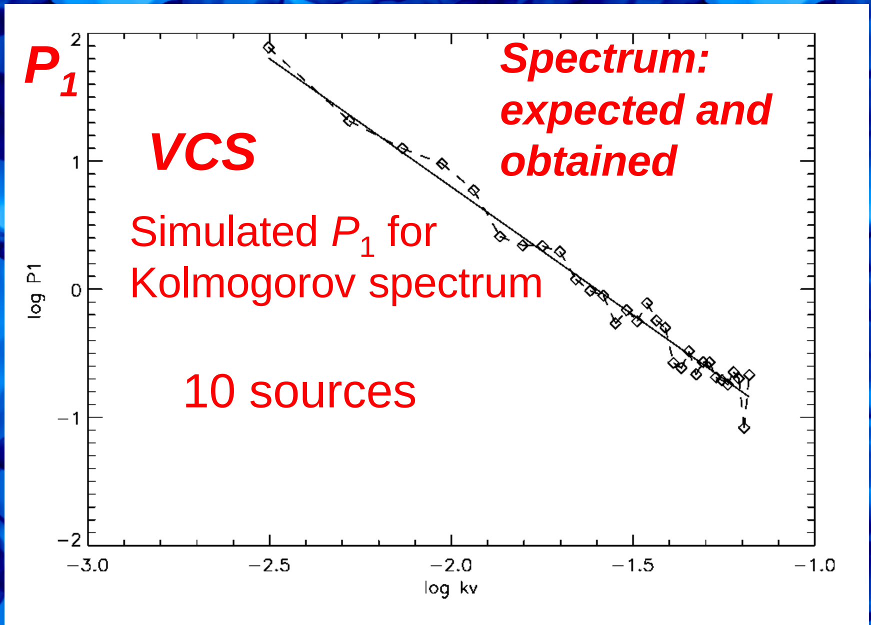

How many spectral measurement are necessary?

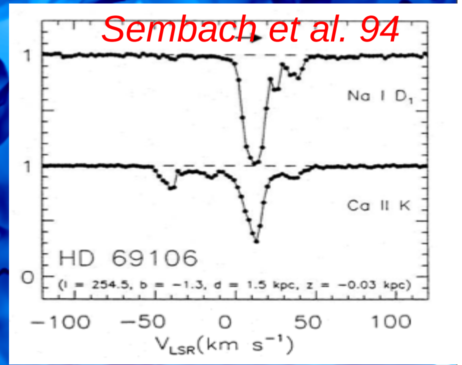

Observations along 5-10 lines of sight are sufficient

One line of sight + galactic shear

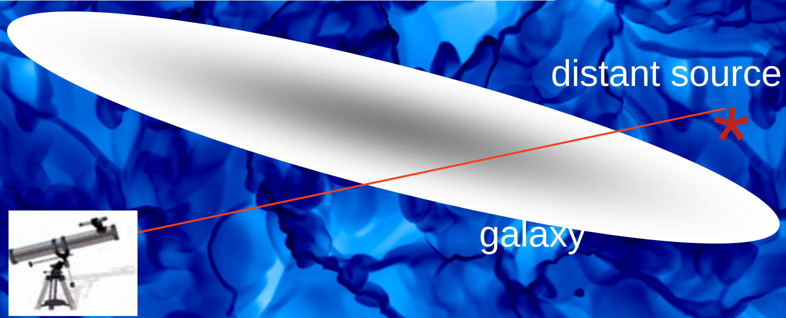

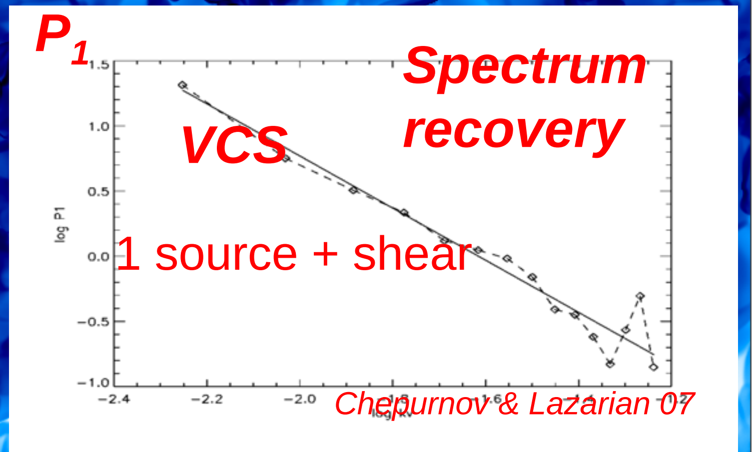

One realization. Δ*v* due to galaxy rotation is 8 times the turbulent line width

Saturated Absorption Lines

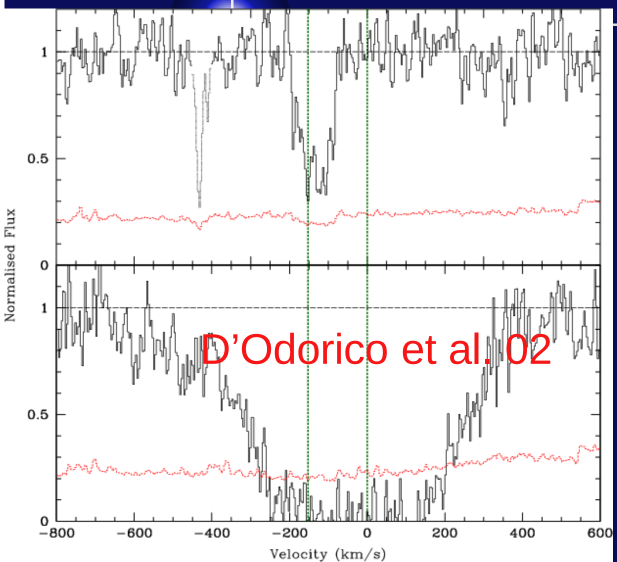

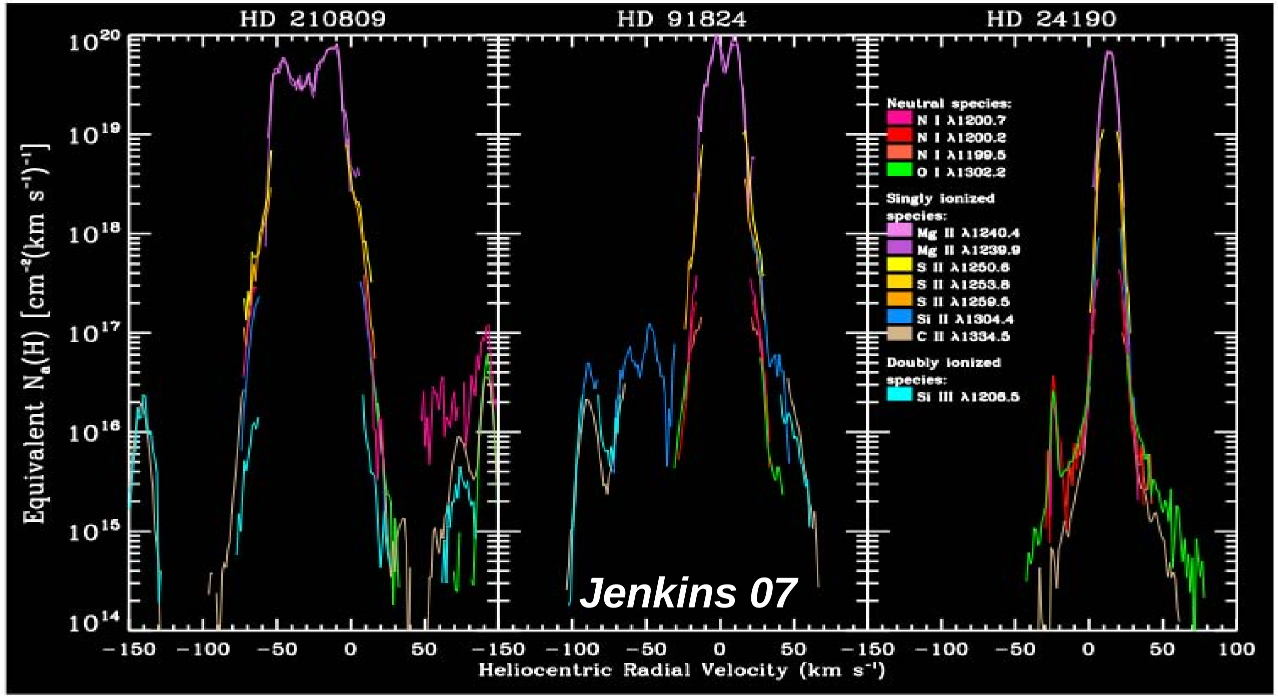

$$\tau(v) = \alpha(\nu_0) \int_0^S dz n(x) H(v - u(x))$$

$$H(v - u(x) - v_{gal}(x)) = \frac{1}{\pi\sqrt{2\pi\beta}} \int dw \frac{a}{(w-v)^2 + a^2}$$ Voigt profile

ΔW Gaussian mask

$$P(k_v) \sim \int_0^S dz \xi(z) \exp\left[\frac{2(a - \Delta W^2 k_v)^2}{D_z(z) + 2\beta + 2\Delta W^2} - k_v^2 \Delta W^2\right] \times \mathrm{Erfc}\left[\frac{a - \Delta W^2 k_v}{\sqrt{D_z(z)/2 + \beta + \Delta W^2}}\right]$$

Higher order structure functions:

$$dD_\tau(v) = \frac{1}{2}\left\langle \left(\tau(v_1 + v) + \tau(v_1 - v) - 2\tau(v_1)\right)^2 \right\rangle$$

Lazarian & Pogosyan 08

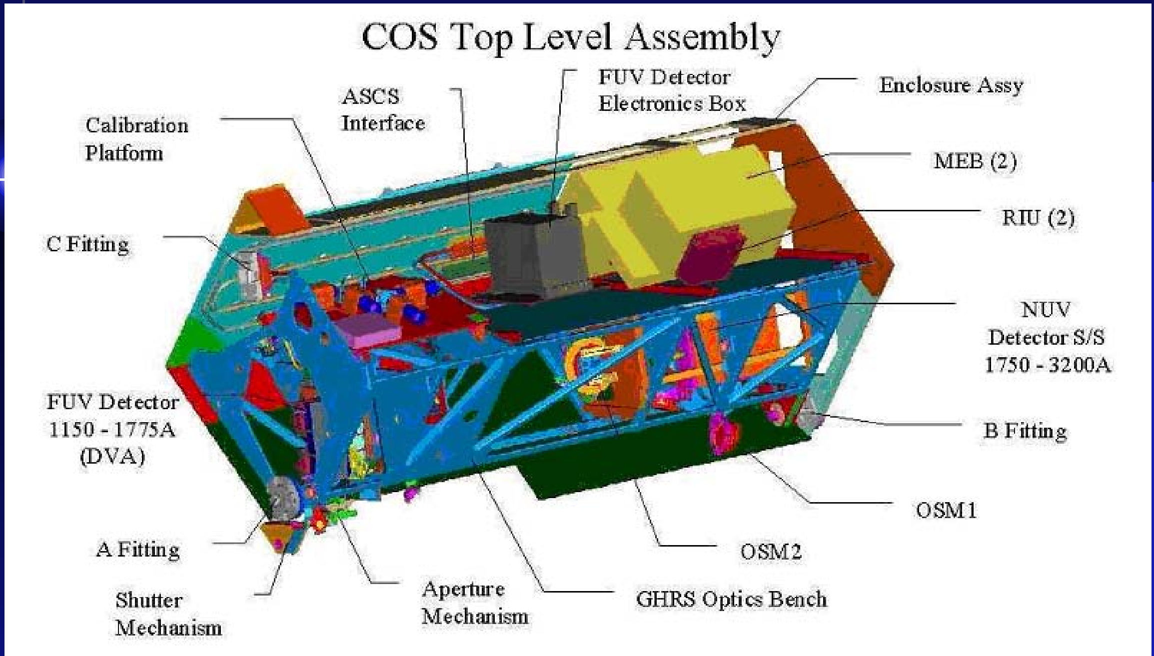
COS Top Level Assembly
Calibration Platform
ASCS Interface
FUV Detector Electronics Box
Enclosure Assy
MEB (2)
RIU (2)
C Fitting
NUV Detector S/S 1750 - 3200A
FUV Detector 1150 - 1775A (DVA)
B Fitting
OSM1
A Fitting
OSM2
Shutter Mechanism
Aperture Mechanism
GHRS Optics Bench